AD-A042 549 AIR FORCE FLIGHT DYNAMICS LAB WRIGHT-PATTERSON AFB OHIO F/G 4/2
A DESCRIPTION OF THE ATMOSPHERIC TURBULENCE ENVIRONMENT DERIVED--ETC(U)
APR 77 P L HASTY

UNCLASSIFIED AFFDL-TR-77-4 NL

1 OF 1
ADA042549

END
DATE FILMED
8-77
DDC

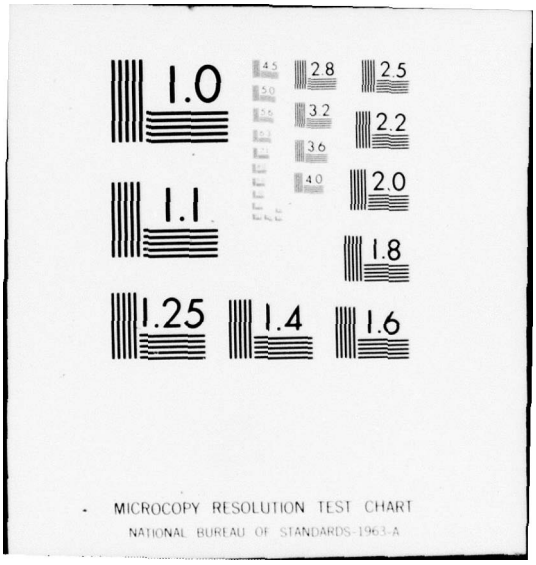
1.0
1.1
1.25
1.4
1.6
1.8
2.0
2.2
2.5
2.8
3.2
3.6
4.0
4.5
5.0
5.6
MICROCOPY RESOLUTION TEST CHART
NATIONAL BUREAU OF STANDARDS-1963-A

AFFDL-TR-77-4

(12)

A DESCRIPTION OF THE ATMOSPHERIC TURBULENCE ENVIRONMENT DERIVED FROM THE CRITICAL ATMOSPHERIC TURBULENCE (ALLCAT) PROGRAM

STRUCTURAL INTEGRITY BRANCH
STRUCTURAL MECHANICS DIVISION

APRIL 1977

TECHNICAL REPORT AFFDL-TR-77-4
FINAL REPORT FOR PERIOD APRIL 1963 - DECEMBER 1973

Approved for public release; distribution unlimited

AIR FORCE FLIGHT DYNAMICS LABORATORY
AIR FORCE WRIGHT AERONAUTICAL LABORATORIES
AIR FORCE SYSTEMS COMMAND
WRIGHT-PATTERSON AIR FORCE BASE, OHIO 45433

NOTICE

When Government drawings, specifications, or other data are used for any purpose other than in connection with a definitely related Government procurement operation, the United States Government thereby incurs no responsibility nor any obligation whatsoever; and the fact that the government may have formulated, furnished, or in any way supplied the said drawings, specifications, or other data, is not to be regarded by implication or otherwise as in any manner licensing the holder or any other person or corporation, or conveying any rights or permission to manufacture, use, or sell any patented invention that may in any way be related thereto.

This report has been reviewed by the Information Office (IO) and is releasable to the National Technical Information Service (NTIS). At NTIS, it will be available to the general public, including foreign nations.

This technical report has been reviewed and is approved for publication.

Paul L. Hasty

PAUL L. HASTY
Project Engineer

R. M. Bader

ROBERT M. BADER, Chief
Structural Integrity Br.
Structural Mechanics Div.

FOR THE COMMANDER

Howard L. Farmer

HOWARD L. FARMER, Col, USAF
Chief, Structural Mechanics Division

Copies of this report should not be returned unless return is required by security considerations, contractual obligations, or notice on a specific document.

AIR FORCE - 28 JUL 77 - 300

UNCLASSIFIED

SECURITY CLASSIFICATION OF THIS PAGE *(When Data Entered)*

REPORT DOCUMENTATION PAGE

READ INSTRUCTIONS BEFORE COMPLETING FORM

1. REPORT NUMBER: AFFDL-TR-77-4	2. GOVT ACCESSION NO.
3. RECIPIENT'S CATALOG NUMBER	
4. TITLE *(and Subtitle)*: A DESCRIPTION OF THE ATMOSPHERIC TURBULENCE ENVIRONMENT DERIVED FROM THE CRITICAL ATMOSPHERIC TURBULENCE (ALLCAT) PROGRAM.	5. TYPE OF REPORT & PERIOD COVERED: Final Report, April 1963 — December 1972
	6. PERFORMING ORG. REPORT NUMBER
7. AUTHOR(s): Paul L. Hasty	8. CONTRACT OR GRANT NUMBER(s): N/A
9. PERFORMING ORGANIZATION NAME AND ADDRESS: Structural Integrity Branch (FBE) Air Force Flight Dynamics Laboratory Wright-Patterson AFB, Ohio 45433	10. PROGRAM ELEMENT, PROJECT, TASK AREA & WORK UNIT NUMBERS: 62201F 1367 01 13
11. CONTROLLING OFFICE NAME AND ADDRESS: Air Force Flight Dynamics Laboratory Wright-Patterson Air Force Base, Ohio 45433	12. REPORT DATE: April 1977
	13. NUMBER OF PAGES: 68 (12) 66 p.
14. MONITORING AGENCY NAME & ADDRESS *(if different from Controlling Office)*	15. SECURITY CLASS. *(of this report)*: UNCLASSIFIED
	15a. DECLASSIFICATION/DOWNGRADING SCHEDULE

16. DISTRIBUTION STATEMENT *(of this Report)*

Approved for public release; distribution unlimited

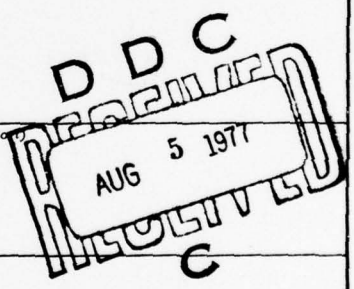

17. DISTRIBUTION STATEMENT *(of the abstract entered in Block 20, if different from Report)*

18. SUPPLEMENTARY NOTES

19. KEY WORDS *(Continue on reverse side if necessary and identify by block number)*

Turbulence
Gusts
Atmospheric Environment
Power Spectral Densities
Gust Velocities

20. ABSTRACT *(Continue on reverse side if necessary and identify by block number)*

This report summarizes the important findings of the individual projects of the Critical Atmospheric Turbulence (ALLCAT) Program. The basic gust parameters are presented for the various altitude regions. Power spectral densities are presented and the results of the investigation are presented in a form useful for gust design procedures. Scale lengths, turbulence intensity, and percentage of flight time in turbulence are presented as a function of altitude.

DD FORM 1 JAN 73 1473 EDITION OF 1 NOV 65 IS OBSOLETE

UNCLASSIFIED

SECURITY CLASSIFICATION OF THIS PAGE *(When Data Entered)*

012079

FOREWORD

This report was prepared by Mr. Paul L. Hasty, Aerospace Engineer in the Loads and Response Prediction Group, Structural Integrity Branch (FBE), of the Structural Mechanics Division, Air Force Flight Dynamics Laboratory at Wright-Patterson Air Force Base, Ohio. The work was performed under Project 1367 "Structural Integrity for Military Aerospace Vehicles", Task 136701 "Structural Flight Loads Data".

The Critical Atmospheric Turbulence (ALLCAT) Program was authorized and funded mostly under the Advanced Development Program 683E. The research was conducted from April 1963 through December 1972.

This report presents a description of gust data obtained from flight test programs. The results are presented in a form useful for the design of aerospace vehicles. This report is a concise summary of the individual projects conducted under the ALLCAT Program or programs directly related to it.

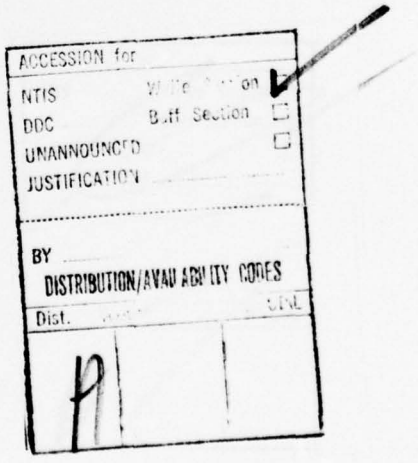

TABLE OF CONTENTS

LIST OF ILLUSTRATIONS

LIST OF ILLUSTRATIONS (Contd)

LIST OF TABLES

LIST OF SYMBOLS

A	Structural response quantity
a	Slope of lift curve
b_1, b_2	Scale parameters for nonsevere and severe turbulence
c	Wing chord
f	Frequency
H	Gust gradient distance
h	Altitude
k	Reduced frequency, $\omega c/2V$
L	Scale of turbulence
m	Slope of power spectral density low wavelength asymtote
N_o	Number of zero crossings per second with positive slope
N	Number of times per second load level x is crossed with positive slope
n	Number of crossings with positive slope
P	Proportion of flight time spent in turbulence
P_1, P_2	Percentage of total flight time spent in nonsevere and severe turbulence
S	Wing area
s	Standard deviation of RMS (λ = 2,000 ft)
t	Time
U_F	Longitudinal gust component measured in the horizontal plane parallel to the average heading of the aircraft over the duration of a run
U_L	Lateral gust component measured in the horizontal plane perpendicular to the average heading of the aircraft over the duration of a run
U_V	Vertical gust component measured perpendicular to the horizontal plane
V	Flight Velocity

LIST OF SYMBOLS (Contd)

u	Longitudinal gust velocity
v	Lateral gust velocity
w	Vertical gust velocity
PSD	Power spectral density
x	Response variable
$\overline{x}$	Minimum value of σ to be classified as turbulence
λ	Wavelength
μ	Mass parameter
ρ	Air density
σ	Total RMS value
σ_c	RMS value associated with cut-off frequency ω_c
σ_t	*Truncated RMS value*
σ_w	RMS value of vertical gust velocity
σ_x	RMS value of variable x
ϕ_w ( )	Power spectrum of vertical gust velocities
ϕ_x ( )	Power spectrum of variable x
ω	Circular frequency
ω_c	Cut-off frequency
Ω	Spatial frequency

SECTION I

INTRODUCTION

The Air Force Flight Dynamics Laboratory conducted a large scale program, the Critical Air Turbulence (ALLCAT) Program, to develop a valid model for the description of the turbulence environment. Large quantities of data have been obtained for developing improved gust criteria, and updating turbulence design criteria. This report presents the significant results of this turbulence investigation and related geophysical, meterological, and climatic conditions. Values of suggested basic turbulence parameters, required for design, are presented. The plan developed to define models of atmospheric turbulence over a wide range of altitudes was as follows:

Program	Altitude (ft) Above Ground
Take-Off and Landing Critical Atmospheric Turbulence (TOLCAT)	0 - 250
Low Level Critical Atmospheric Turbulence (LO-LOCAT)	250 - 1000
Medium Altitude Critical Atmospheric Turbulence (MEDCAT)	20,000 - 40,000
High Altitude Critical Atmospheric Turbulence (HICAT)	40,000 - 70,000

SECTION II

PROJECT TOLCAT

Turbulence encountered during take-off and landing can present serious hazards to aircraft. Both temporal and spatial descriptions of turbulence are required for design problems. The Take-Off and Landing Critical Atmosphereic Turbulence Project (TOLCAT) was initiated to develop experimentally the necessary knowledge of turbulence in the atmospheric boundary layer, its dependence on height, terrain features, meteorological conditions, and to determine the interrelationship between temporal and spatial characteristics.

An experimental investigation was conducted to develop optimum methods and techniques for data acquisition and analysis required to define the atmospheric boundary layer turbulence environment. The investigation was specifically designed for V/STOL aircraft flight control and stability studies and to develop valid structural design criteria. Measurements of turbulence were made from various arrays of sensors mounted on towers to demonstrate methods of describing the temporal and spatial characteristics of turbulence. The towers were located near Hanford, Washington. Measurement and data reduction techniques for sonic and three-propeller anemometers were optimized to assure accurate measurements of the vertical and two horizontal wind components from the sensors. Table 1 summarizes the experimental arrays.

Experiments were conducted from a T-shaped array consisting of four sensors mounted on booms to simulate two wing positions (9 meters apart), fuselage position, and tail position (6 meters from wings) on an aircraft and thereby compute correlations for various gust and shear combinations to which an aircraft would respond.

On another tower, six sensors were spaced logarithmically along a vertical line. Sonic anemometers were installed at 60, 15, and 7.5 meters, and Gillanemometers were installed at 30, 3.75, and 1.88 meters above the ground.

TABLE 1

EXPERIMENTAL ARRAYS

Number	Number of Towers	Height (Meters)	Spacing
1	4	58	Horizontal, four sensors, one on each tower which are equally spaced (223 meters)
2	1	58	Horizontal, T-shaped, two sensors 9 meters apart and two sensors 6 meters apart - simulate aircraft
3	8	4	Horizontal, eight sensors, log spaced over total of 1023 meters
4	1	12	Horizontal, six sensors, 1.5 meters apart
5	1	1.88 to 60	Vertical, six sensors, log spaced
6	9	15	Horizontal, L-shaped, seven sensors log spaced on principal leg (128 meters) and sensors at 12 and 60 meters on short leg
7	9	30	Same as Array 6
8	1	131	Single sensor

An L-shaped array included nine sensors horizontally dispersed. The principal leg of the L consisted of seven logarithmically spaced positions with separation distances between consecutive sensors varying from 4 to 128 meters. The purpose of this line of sensors was to make possible the comparison of time and space analyses when the wind blew from various azimuth angles to the principal line. The short leg of the L-array had two positions, 12 and 60 meters from the origin. The purpose of the short line of sensors was to make possible comparison of correlations in two directions at 12 and 60 meters. The same tower locations were used for both the 15-meter and the 30-meter L-arrays. The only difference was the heights at which the sensors were mounted. The purpose was again to obtain spatial correlations and cross spectra to compare with time series analysis.

In the final experiment, a single sensor was mounted atop the 125-meter tower in order to obtain samples of data at elevations above the surface layer, where the existing turbulence is related less to the local wind shear and more to convection and vertical transport of turbulence from below.

Several tests were conducted with the sensors in each of the arrays described above. A list of twelve data segments chosen for analysis on the basis of their high quality is given in Table 2. In the first column, the first digit gives the array number (from Table 1) and second digit gives a serial number identifying the particular test within the series.

Both analog and field digital magnetic tape recording options were demonstrated to provide flexibility in measurement array configurations and to optimize recording capabilities for a variety of measurement requirements. Data reduction, processing, and analysis techniques were developed. The detailed results are presented in References 1 and 2.

TABLE 2

TESTS ANALYZED FOR TOLCAT

Test No.	Date	Time Segment	Stability	Mean Wind Direction (Deg)	Mean Wind Speed (mps)	Mean Wind Height (m)
15	681202	1345-1426	Slightly Stable	212	8	58
22	690925	1552-1647	Slightly Stable	296	9	58
51a	700720	1537-1605	Unstable	320	9	60*
51b	700720	1619-1647	Unstable	304	10	60*
56	700723	2143-2238	Stable	301	12	60*
58	700728	1910-2005	Neutral	303	9	60*
63	710119	1323-1351	Slightly Stable	300	6	15
71	710303	1316-1344	Unstable	243	14	30
73	710324	0945-1013	Unstable	303	7	30
74	710326	1013-1059	Unstable	200	13	30
83	710607	1143-1224	Unstable	297	5	131
85	710621	1059-1154	Unstable	50	3.6	131

*Turbulence measurements were taken at lower heights

Some experimental data were collected from tower arrays as shown in Table 1.

Only some general conclusions can be stated as a result of the TOLCAT investigation. Initial studies of Taylor's hypothesis showed that autocorrelation functions scaled by the mean wind speed to the expected spatial functions agreed quite well with the measured spatial correlations. This hypothesis states that the space and time autocorrelations (or equivalently spectra) are equal (with the transformation $x_i = \bar{U}t$). $\bar{U}$ is the speed of the airplane with respect to the atmosphere, and x_i refers to the three space directions. The use of the hypothesis allows one to obtain information by using one probe and doing analysis in time, instead of using two probes and doing analysis in space. The translation of time series spectra to that experienced by an aircraft holds only for the case where the aircraft flies in the direction of the wind.

Modeling of turbulence, appropriate to take-off and landing problems, will require an extensive measurement and analysis effort to follow this development phase.

SECTION III

PROJECT LO-LOCAT

The LO-LOCAT Program was established to determine the turbulence environment below 1000 feet above the ground utilizing statistically representative samples of turbulence data obtained over a wide range of meteorological, topographical, seasonal, and time-of-day conditions. The following major areas were studied: probabilities of encountering given levels of turbulence intensity, frequency analysis of atmospheric turbulence utilizing the power spectra method, correlation of atmospheric turbulence with meteorological and geophysical conditions, and associated forecasting techniques. The basic information concerning the three phases of the LO-LOCAT Program are presented in Table 3 from Reference 3.

The LO-LOCAT data consist exclusively of clear air data. No storm flights are included. During the program, specific routes were flown on a scheduled basis without regard to the amount of turbulence predicted. The data sample can be considered a random sample of the gust environment of the atmosphere during nonstorm conditions. The model used to represent atmospheric turbulence is considered to be made up of discrete patches of turbulence of different intensity, where each patch is assumed to be Gaussian and stationary. If a single stationary, Gaussian patch is considered, the average number of gust peaks per unit distance which exceed a given level of vertical velocity is given by

$$N(w) = N_o e^{-\left(\frac{w^2}{2\sigma^2}\right)}$$

(This is true for one particular turbulence spectrum). N_o is the average number of times per unit distance that the gust velocity function crosses the value zero with positive slope.

TABLE 3

BASIC LO-LOCAT INFORMATION

	Phases I & II	Phase III
Aircraft used to obtain data	4 C-131's	1 T-33
Flight period	9-15-66 - 12-20-67	8-16-68 - 6-30-69
Number of turbulence data flights	1,244	299
Low altitude turbulence data samples	8,871	1,938
BREN tower samples	0	8
Thunderstorm turbulence samples	0	55
Wake turbulence samples	0	46
Turbulence sample average length	21 mi.	32 mi.
Turbulence sample average time interval	5.5 min.	4.5 min.
Average turbulence PSD wavelength band	33 - 7,980 feet	63 - 15,100 feet
Aircraft average ground speed	332 fps	630 fps
u time series samples analyzed statistically	6,553	1,730
v time series samples analyzed statistically	6,270	1,709
w time series samples analyzed statistically	6,508	1,716
u non-contour samples	1,113	0
v non-contour samples	1,091	0
w non-contour samples	1,118	0
u rms values analyzed statistically	7,670	1,762

TABLE 3 (Contd)

	Phases I & II	Phase III
v rms values analyzed statistically	6,621	1,740
w rms values analyzed statistically	7,630	1,746
Gust velocity samples for which spectra were calculated	1,775	904
Homogeneous u spectra analyzed	1,272	591
Homogeneous v spectra analyzed	1,061	524
Homogeneous w spectra analyzed	1,259	496
u spectra obtained during non-contour flight	207	0
v spectra obtained during non-contour flight	200	0
w spectra obtained during non-contour flight	210	0
Gust velocity time series samples per turbulence sample	33,000	27,000
Time interval - spectra calculations	0.01 sec.	0.02 sec.
Gust velocity samples in spectra calculations	33,000	13,500
Frequency interval - spectra calculations	0.0416 cps	0.0416 cps
Nyquist frequency	50 cps	25 cps
Number of frequency estimates PSD	1,200	600
Miles covered recording acceptable turbulence data	135,900	55,750
Hours of acceptable turbulence data	600	130
Spectrum degrees of freedom - individual samples	55	45

For the complete model, the equations for N(w) become

$$N(w) = \frac{1}{d}\left[d_1 N_o e^{-\frac{w^2}{2\sigma_1^2}} + d_2 N_o e^{-\frac{w^2}{2\sigma_2^2}} + \ldots\right]$$

$$= N_o\left[P_1 e^{-\frac{w^2}{2\sigma_1^2}} + P_2 e^{-\frac{w^2}{2\sigma_2^2}} + \ldots\right]$$

d is the total distance traveled by an aircraft in turbulence and d_1 is the distance traveled in turbulence of intensity σ_1. For the limiting case of a continuous variation in the rms value σ, this equation becomes

$$N(w) = N_o \int_0^\infty P(\sigma) e^{-\frac{w^2}{2\sigma^2}} d\sigma$$

where $p(\sigma)$ = probability density of σ

In a study performed by the University of Dayton Research Institute (Reference 4), it was found that the cumulative distribution of peak count exceedance F(x) is reasonably well represented by

$$F(x) = P_1 e^{-x/b_1} + P_2 e^{-x/b_2}$$

and the density function by

$$f(x) = \frac{P_1}{b_1} e^{-x/b_1} + \frac{P_2}{b_2} e^{-x/b_2}$$

For the LO-LOCAT data, P_1 and P_2 represent the percentage of total flight time spent in nonsevere and severe turbulence. b_1 and b_2

are turbulence scale parameters for the individual probability distributions of σ_w. Using the equation

$$F(x) = \frac{N(x)}{N_o} = P_1 e^{-x/b_1} + P_2 e^{-x/b_2}$$

the LnF(x) was represented by a quadratic of the form

$$LnF(x) = A + Bx + Cx^2$$

This transformation requires a representation of P_1, P_2, b_1 and b_2 in terms of A, B, and C. If C is negative this indicates that the cumulative probability function is concave down. The best fit that can be made to such data is to define $P_1 = 1$ and $P_2 = 0$. The LnF(x) reduces to the form: $LnF(x) = A-mx$, where $m = 1/b_1$. When C is positive, P_1, P_2, b_1 and b_2 are determined from the coefficients of the equation:

$$LnF(x) = A + Bx + Cx^2$$

b_1 is defined as the negative reciprocal of the slope of $LnF(x) = B + 2\,CX$; at $x = 0$, the slope = B and $b_1 = 1/B$. To determine b_2, the negative reciprocal of the slope of LnF(x), the point of transition between the influences of the first and second terms of Equation

$$F(x) = P_1 e^{-x/b_1} + P_2 e^{-x/b_2}$$

is chosen as $x_c = x_m/2$ where x_m is the maximum gust velocity encountered.

$$b_2 = -\frac{1}{B + 3\,Cx_c} = -\frac{1}{B + 3\,C\frac{x_m}{2}}$$

$$-1/b_2 = B + 3\,C\frac{x_m}{2}$$

Recommendations, from Reference 4, are given for P_1, P_2, b_1, b_2 and the von Karman L for the 0-1000 ft altitude region in nonstorm flight conditions

$$P_1 \exp - \frac{x_c}{b_1} + P_2 \exp - \frac{x_c}{b_2} = \exp(Bx_c + Cx_c^2)$$

The section gives recommendations for P_1, P_2, b_1, b_2 and the von Karman L for the 0-1000 ft altitude region in nonstorm flight conditions (Reference 4). Also, probability of exceedance curves are presented for various environmental conditions. Figure 1 shows the cumulative exceedance curves for the Phases I and II and Phase III data. For Phases I and II a maximum gust of 66 ft/sec in the vertical component was observed during a noncontour flight. During Phase II the maximum gust was 76 ft/sec over high mountains. The cumulative exceedance curves for all Phases I and II flight legs at 250 ft and for all legs at 750 ft are presented in Figure 2. Little difference is seen between the two curves. The cumulative probability curves of each component of Phase I and Phase II data is shown in Figure 3. Similar results were obtained for the Phase III data

The cumulative probability exceedance curves for all Phase III flight legs have been shown to be considerably larger than those of Phases I and II. If one considers only those Phase III legs not flown over high mountains, there is good agreement with Phases I and II. Hence, it was decided to combine Phase III data, excluding high mountain data, with all of Phases I and II. Figure 4 shows the cumulative probability curve for all of Phases I, II and III, excluding high mountain data. The corresponding P's and b's are listed; Phase III high mountain data are also shown. A decomposition of the data of Figure 4 into legs flown in very stable air and those not flown in very stable air is given in Figure 5. Table 4 summarizes the recommended P's and b's for the 0-1000 ft altitude range. The exceedance curves of Figure 4 have been presented by longitudinal, lateral, and vertical components in Figures 6 and 7.

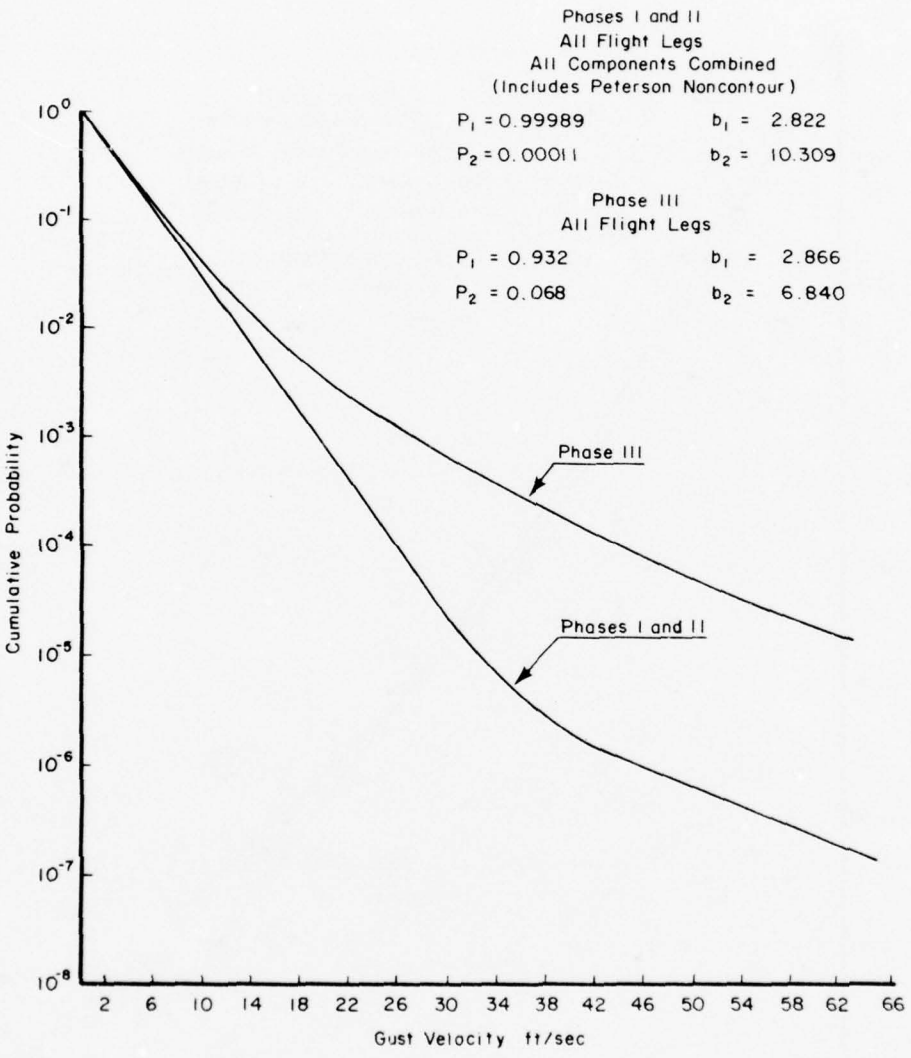

Figure 1. Cumulative Probability of Exceedance, Phases I and II vs. Phase III

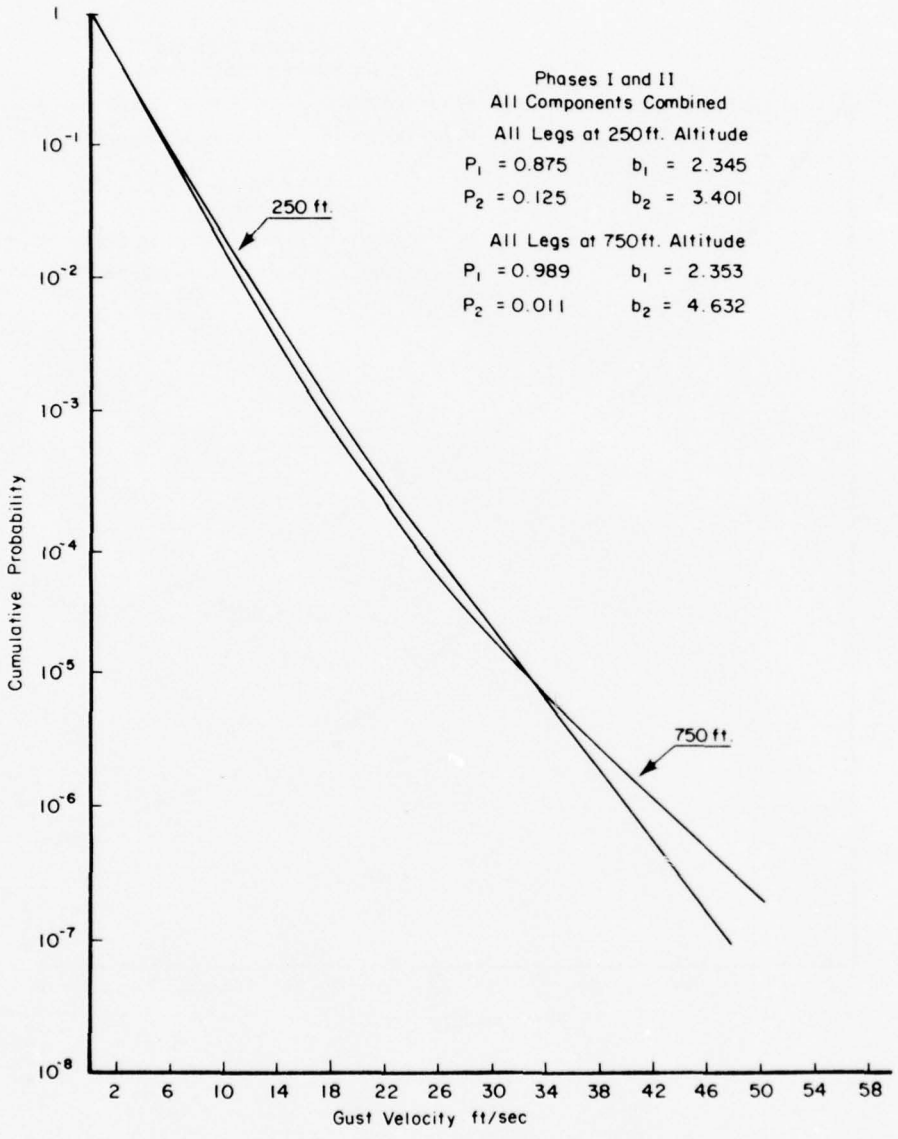

Figure 2. Cumulative Probability of Exceedance, 250 ft and 750 ft Altitude

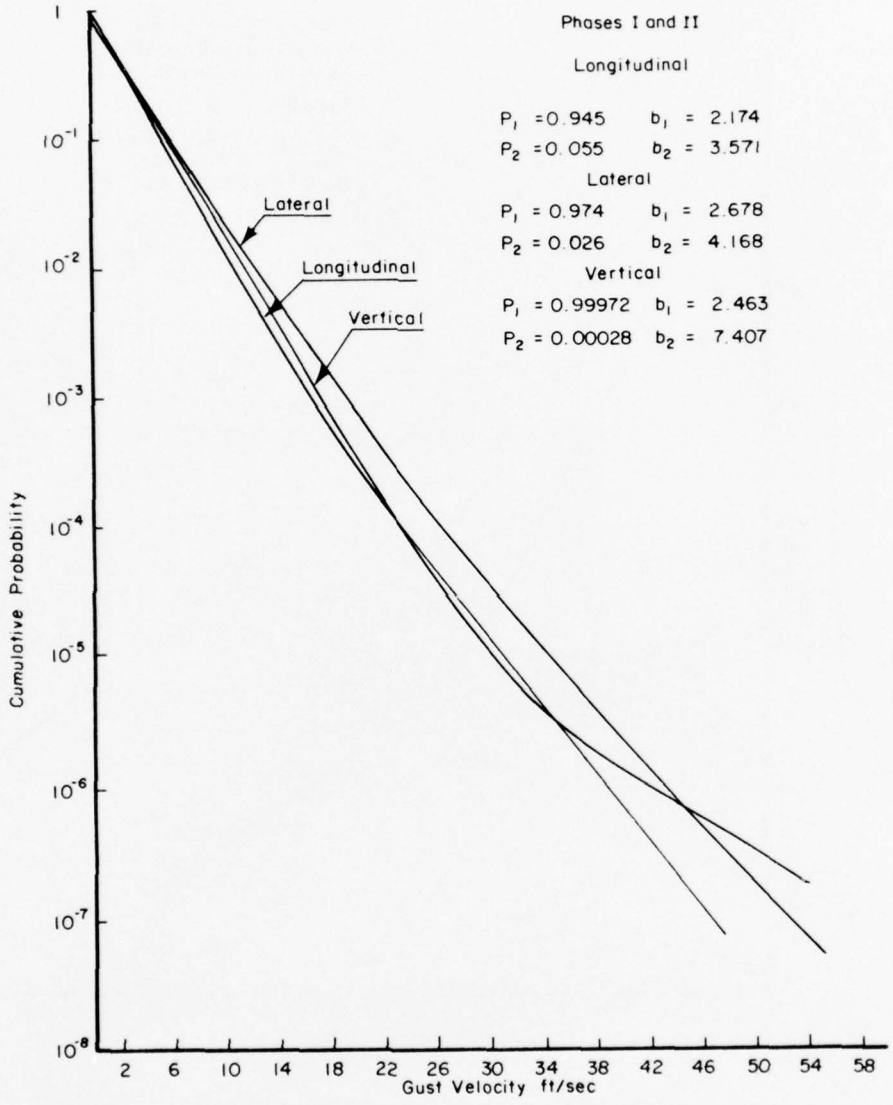

Figure 3. Cumulative Probability of Exceedance Phases I and II, Longitudinal, Lateral, and Vertical Components

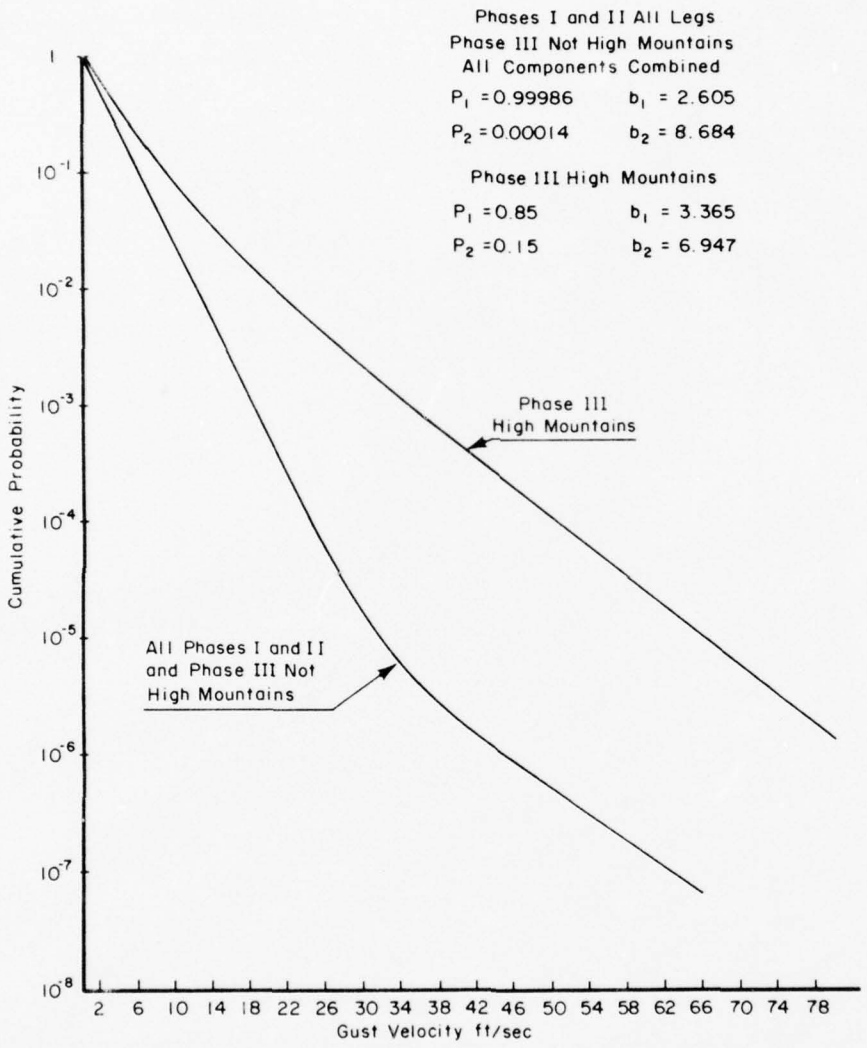

Figure 4. Cumulative Probability of Exceedance for Phases I and II and Not High Mountains Phase III Legs; Phase III High Mountains Legs

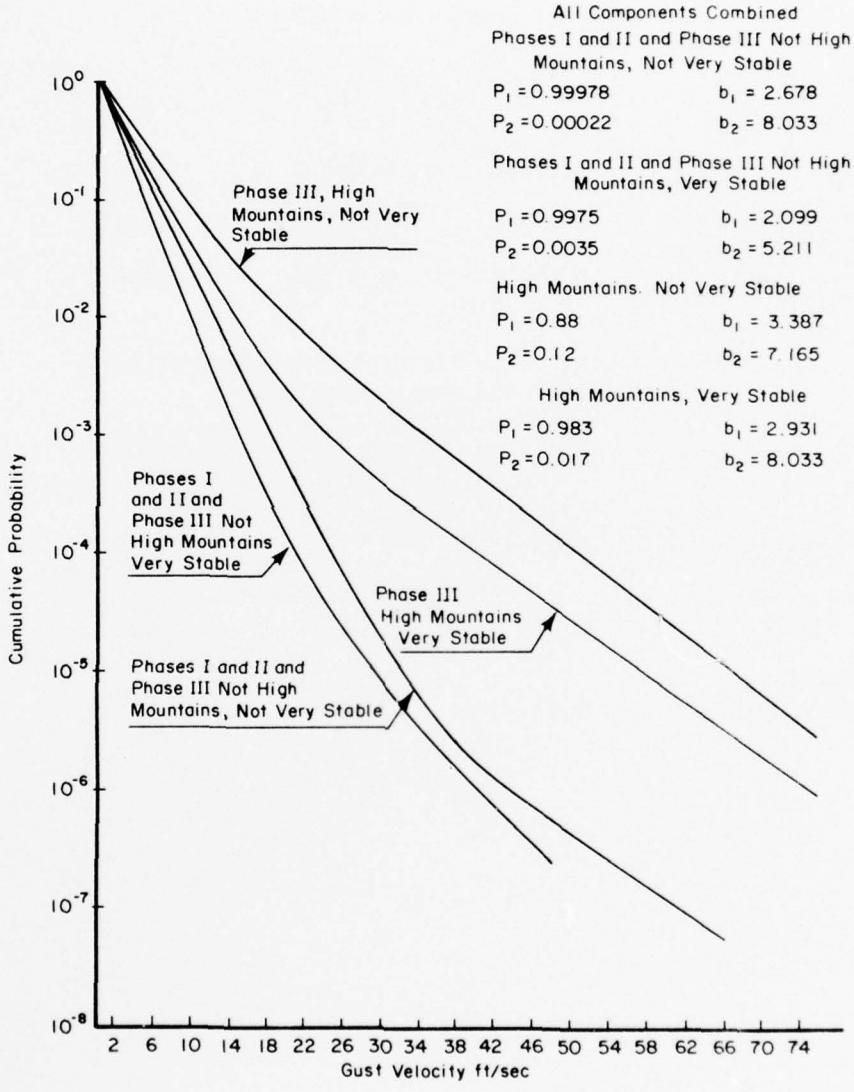

Figure 5. Cumulative Probability of Exceedance, Very Stable-vs-Not Very Stable Legs

TABLE 4

RECOMMENDED P's AND b's FOR 0-1000 FOOT ALTITUDE
NONSTORM CONDITION

Data Includes All Phases I and II Legs
and Phase III Legs Not Over High Mountains

All Components Combined

	P_1	P_2	b_1	b_2
All Legs	0.99986	0.00014	2.605	8.684
Very Stable	0.99750	0.00250	2.099	5.211
Not Very Stable	0.99978	0.00022	2.678	8.033

Data Includes Phase III High Mountain Legs Only
All Components Combined

	P_1	P_2	b_1	b_2
High Mountains	0.85	0.15	3.365	6.947
High Mountains Very Stable	0.983	0.017	2.931	8.033
High Mountains Not Very Stable	0.88	0.12	3.387	7.165

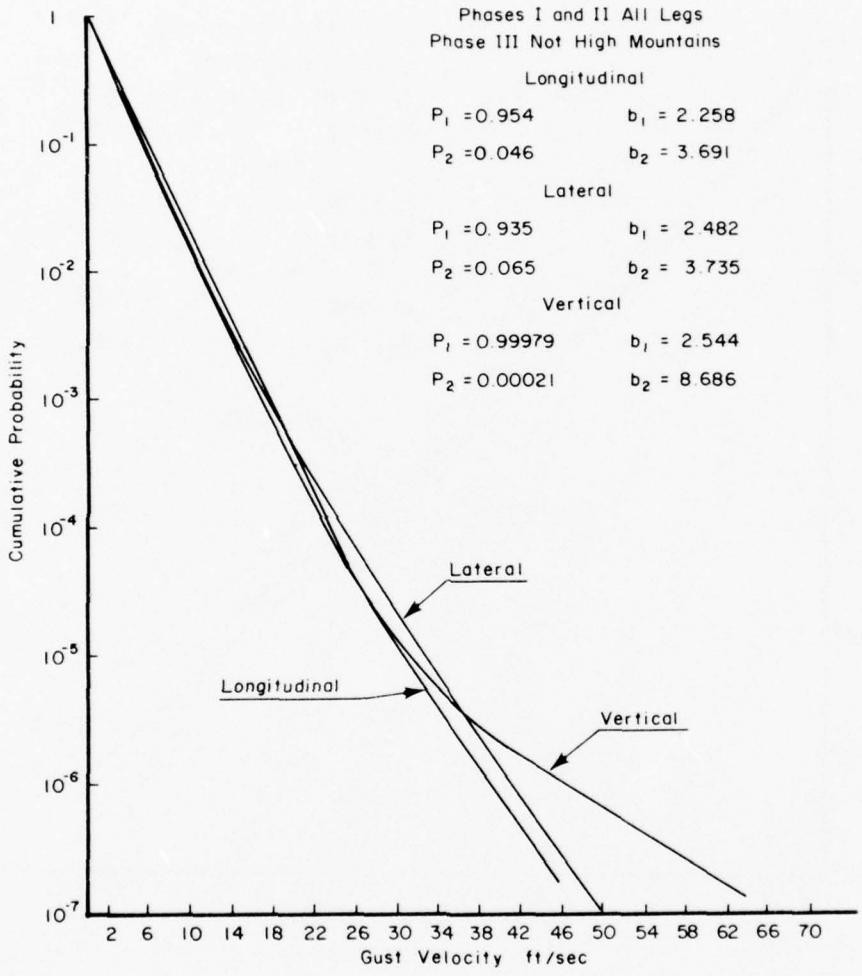

Figure 6. Cumulative Probability of Exceedance for Phases I and II and Not High Mountains Phase III Legs by Component

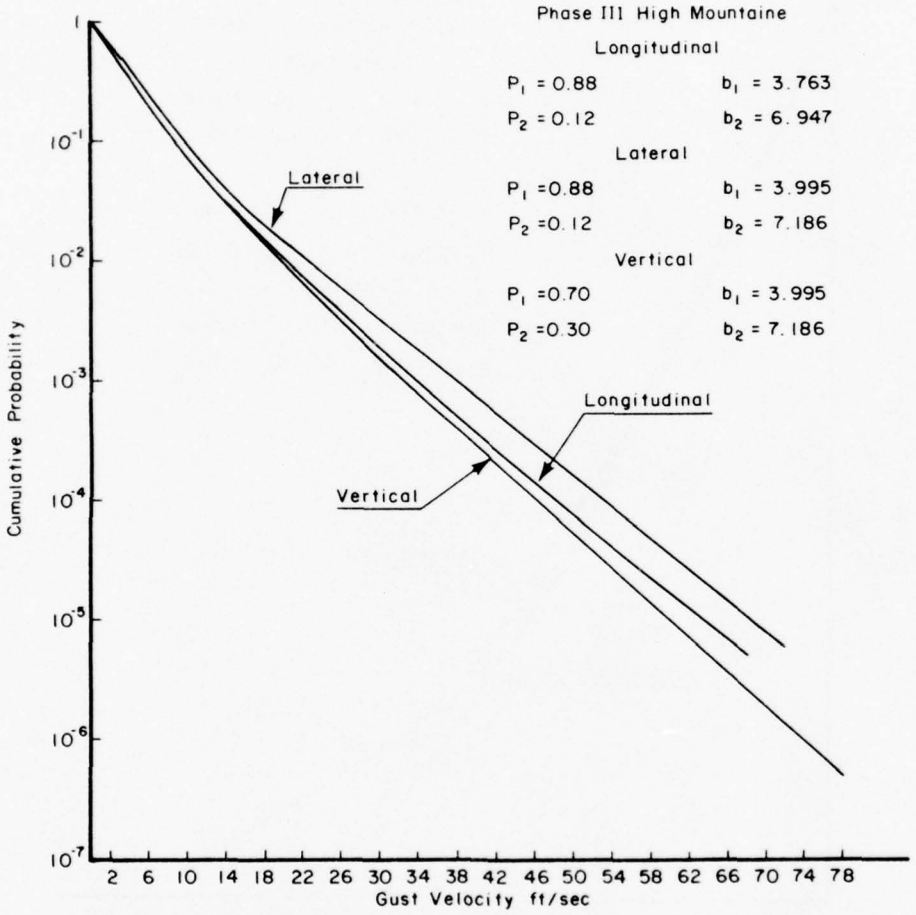

Figure 7. Cumulative Probability of Exceedance for Phase III High Mountains Legs by Component

The von Karman L's were obtained for all components of the data and the results are presented in Table 5.

A complete record of the LO-LOCAT Program is presented in References 3 through 7.

TABLE 5

MEAN VON KARMAN L's

Phases I and II

Component	Altitude 250 ft.	Altitude 750 ft.
All Components	342	442
Longitudinal Component	368	411
Lateral Component	361	465
Vertical Component	302	449

Phase III

Component	Terrain High Mountains	Terrain Not High Mountains
All Components	704	564
Longitudinal Component	813	687
Lateral Component	704	555
Vertical Component	579	430

SECTION IV

PROJECT MEDCAT

The objective of the MEDCAT Project was to measure and characterize the turbulence in the 20,000-40,000 ft regime. Flights were planned to penetrate those regions predicted as being most likely to contain turbulence. Hence the percentage of time in turbulence experienced during this program is not a valid estimate of an expected time in turbulence during operational missions.

F-106 and F-100 aircraft flew a total of 284 flights which resulted in 121 hours and 288 hours respectively, of flight time in search for turbulence. A complete description of this program and an analysis of the data collected is given in Reference 8. The primary characterizations of the turbulence encountered are expressed in terms of power spectral densities and counts of true gust velocities of the three turbulence components. The wave lengths represented in the power spectral densities have a lower limit of 100 ft (approximately 8 cps) and a maximum limit of 1/20 of the length of the processed run.

After the quality evaluation of the data, none of the F-106 flights were processed. Only 25 flights were processed from the F-100 data bank, those judged to contain turbulence intensity yielding rms values greater than 1.5 ft/sec. Any conclusions concerning the character of turbulence from the MEDCAT data sample must be made with reservations. Accuracy limitations precluded the possibility of removing all aircraft motions from the time gust computations, particularly that characteristic ratio of the F-100 aircraft due to the short period longitudinal and dutch roll modes. However, conclusions of a general nature can be drawn.

Estimates of the following basic parameters are required from the collected data to use the theoretical models which describe power spectral densities of atmospheric turbulence: the slope, m (of a log-log plot of the power spectral density) in the short wave-length region; the scale of turbulence, L; and the mean square value of the true gust velocities, σ^2. From an analysis of the MEDCAT data it was concluded

that the scale of turbulence L is > 2000 ft, m = -1.83 for the vertical component, and the most probable σ values were 4.5 ft/sec. for the lateral component and 3.5 ft/sec. for the vertical.

In the F-100 data sample, less than 1% of the time was in turbulence for which at least one component had an rms value greater than 1.5 ft/sec. The data also indicate that the turbulence is not isotropic.

Typical power spectral densities (PSD) for the lateral and vertical components have shapes represented by the curves of Figure 8. The aircraft motion distortions are not as pronounced in the vertical component as in the lateral but on some of the vertical spectra peaks and valleys quite similar to that of the lateral component were present.

The plots of the power spectral densities of true gust velocity components on log-log paper typically exhibit a straight line portion in the short wave length region of the curves. The slope of this straight line portion provides an estimate of the exponent from assumed turbulence models in this inertial subrange of the power spectral density. There was considerable variation in slope between the individual runs. The slopes of the lateral component ranged from -1.2 to -2.2 with a mean of -1.77, while those of the vertical component ranged from -1.0 to -1.9 with a mean of -1.41. Histograms of these slopes are presented in Figure 9.

In order to arrive at one spectrum for use in model development and design criteria, average power spectral densities were computed for the lateral and vertical components. Each power spectral density was first normalized by dividing the abscissa by σ^2_{2000}. σ^2_{2000} is the rms associated with cut-off wavelength of 2000 feet. A weighted average of these normalized spectra was then obtained, the weighting factors being

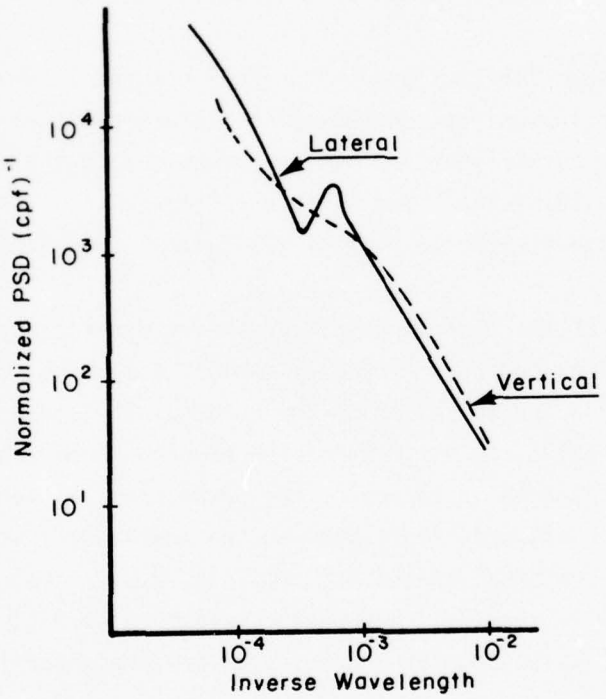

Figure 8. Sketches of Typical Vertical and Lateral Power Spectral Densities of a Long Turbulence Run

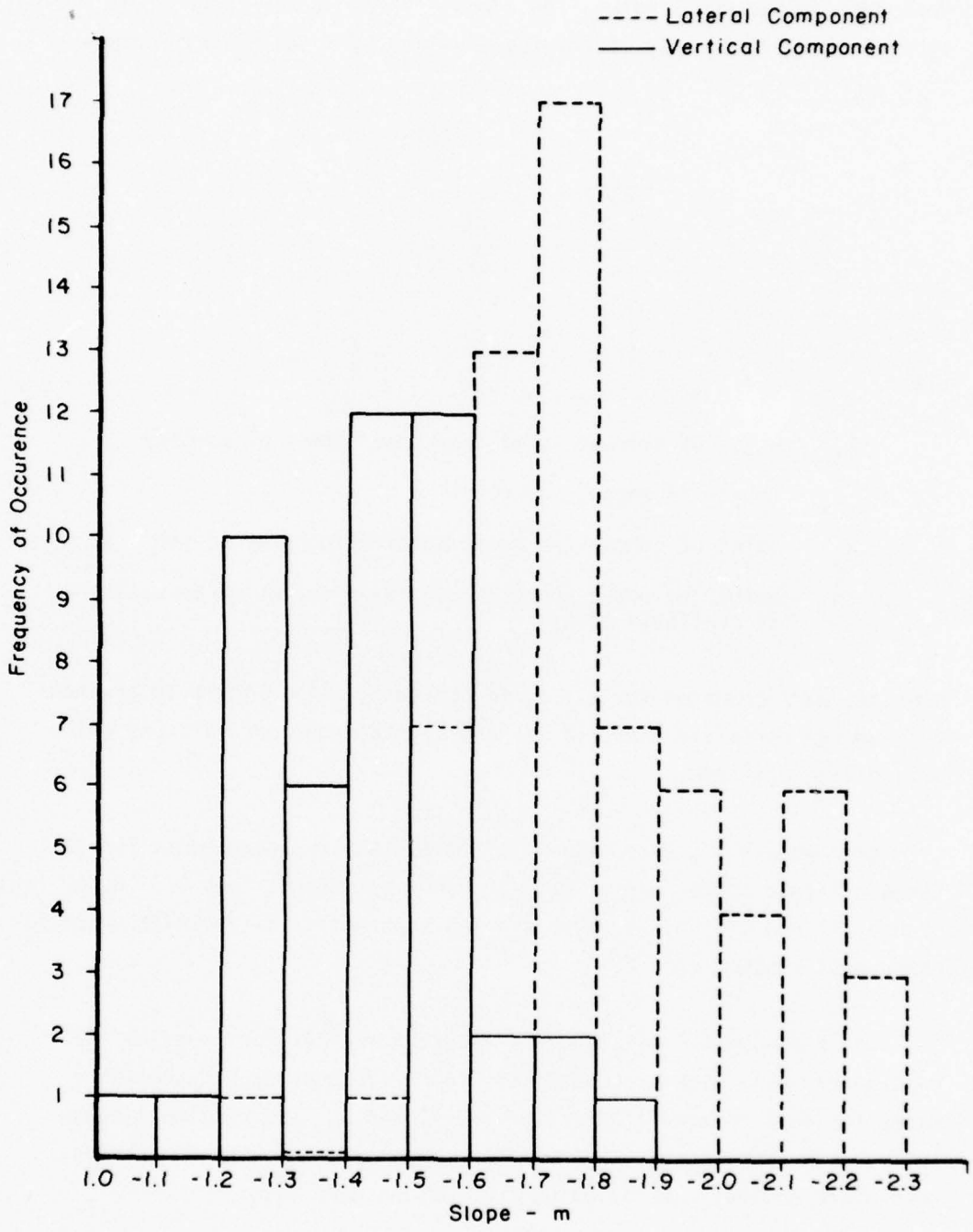

Figure 9. Histogram of Spectral Slopes

dependent on the run length. The average spectrum was computed at approximately 25 equally spaced log k values by means of the formula

$$\overline{\phi(k_j)} = \frac{\sum_{i=1}^{n_j} T_i \phi_i(k_j)}{\sum_{i=1}^{n_j} T_i}$$

where

$\phi(k_j)$ = value of average normalized power spectral density

T_i = length in seconds of run i

$\phi_i(k_j)$ = value of normalized power spectral density of run i at k_j

n_j = number of power spectral densities for which an estimate is available at λ_j

Averages were computed for all λ_j for which $n_j \geq 4$. Figure 10 presents the average normalized spectra for all lateral and vertical runs which met editing criteria.

Average spectra were also obtained for the two components for the three altitude bands, $h < 30{,}000$, $30{,}000 < h < 35{,}000$, and $h > 35{,}000$ feet. Figures 11 and 12 present these average spectra for lateral and vertical components respectively.

The peak count cumulative distribution for all runs meeting the editing criteria were processed into composite peak count exceedance rates for each component direction, u, v, and w. The resultant cumulative peak count rates are shown in Figure 13. From the cumulative rate distributions the following conclusions were made:

(a) Clear air turbulence is composed of more than one rms intensity for each component.

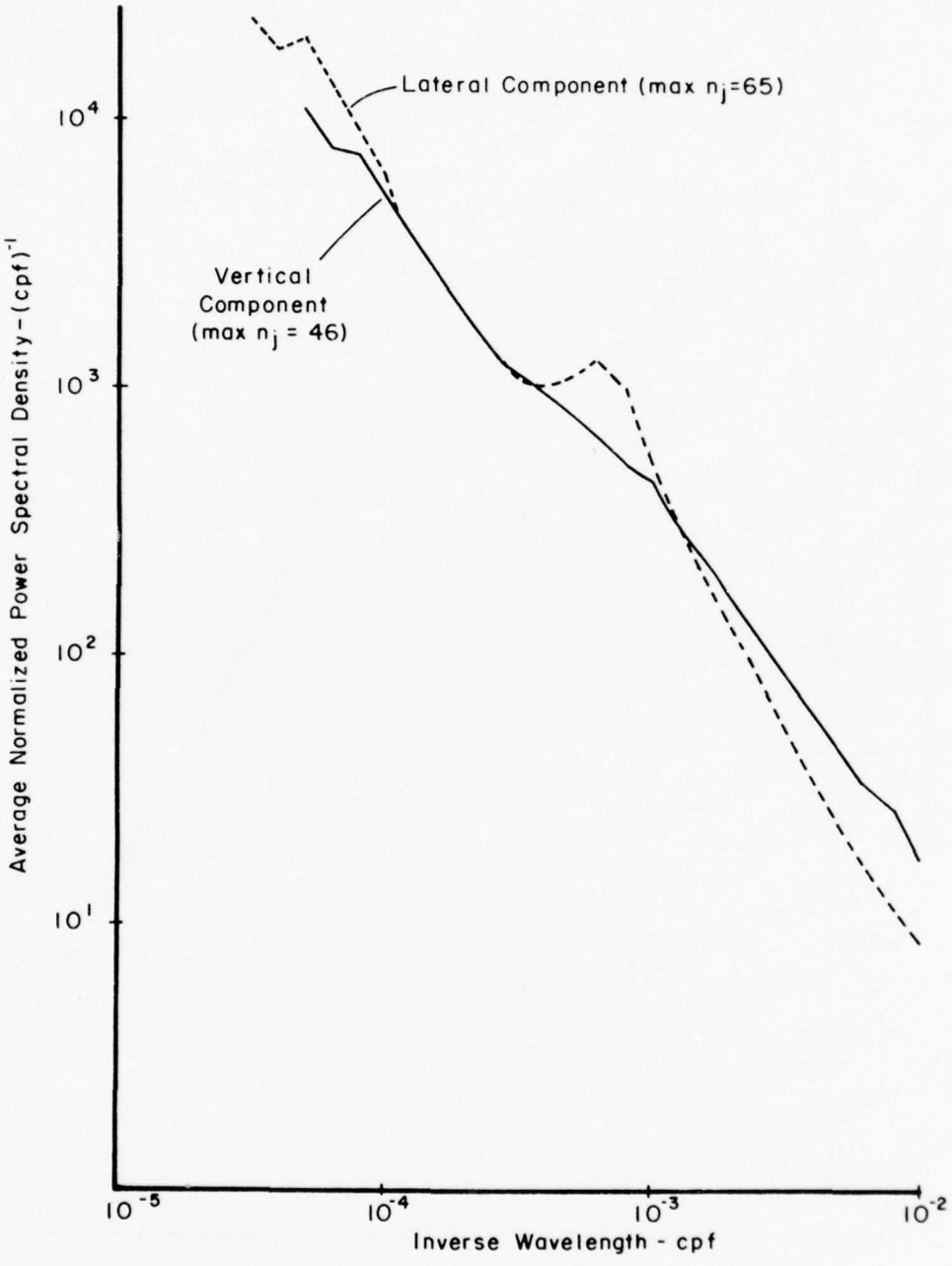

Figure 10. Average Power Spectral Densities Normalized by σ^2_{2000}

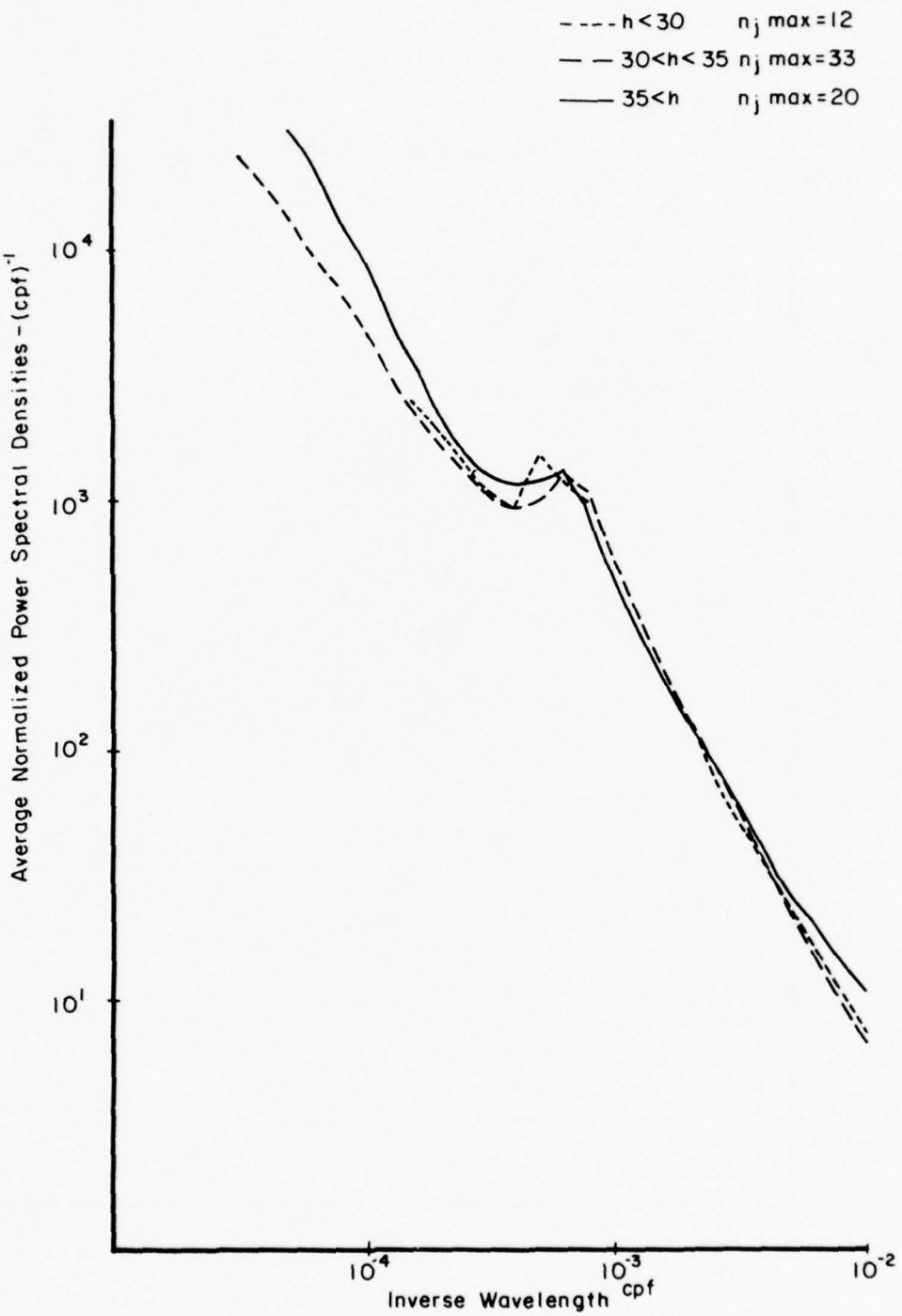

Figure 11. Average Lateral Spectra Normalized by σ^2_{2000} for Three Altitude Bands

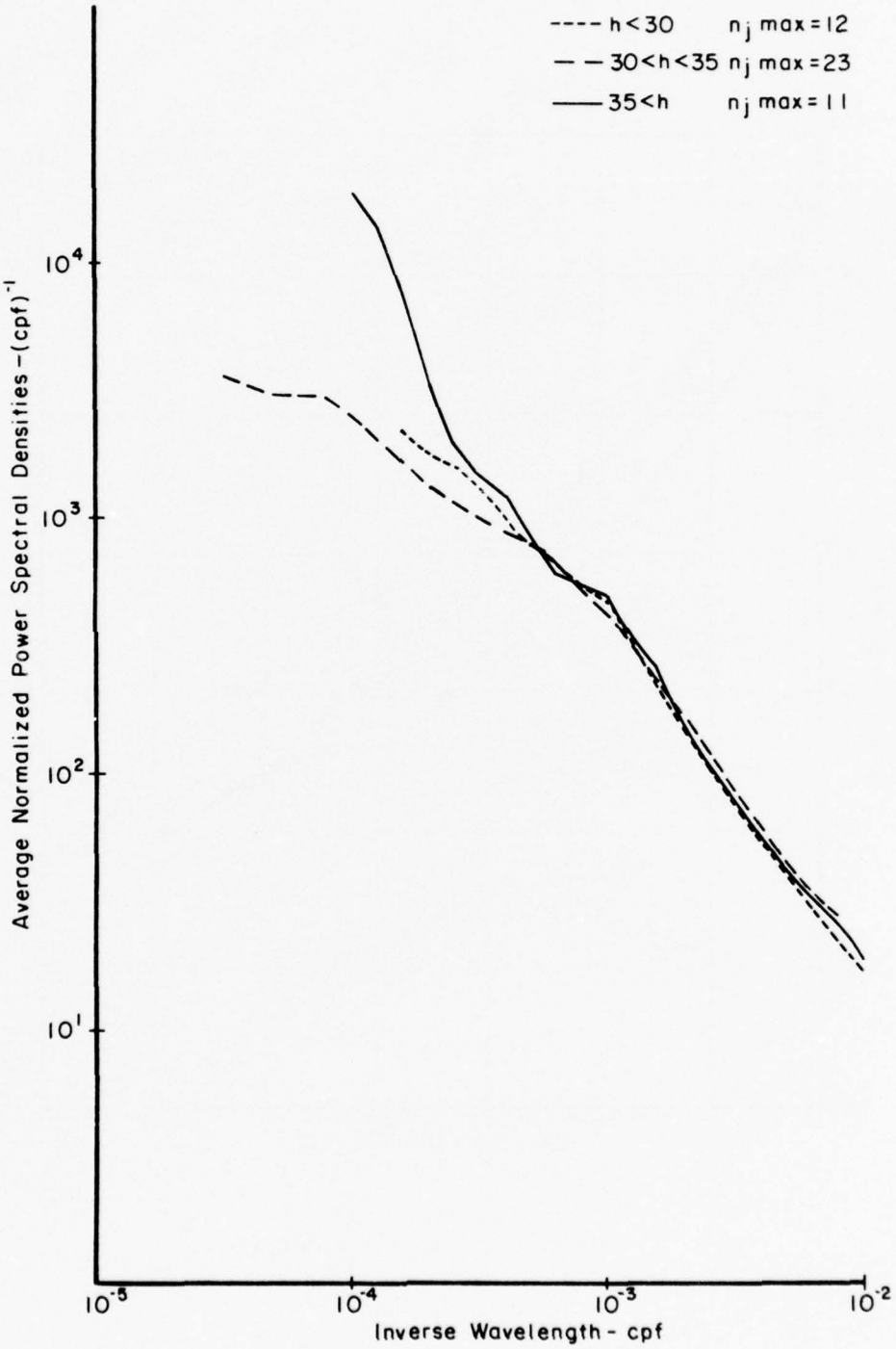

Figure 12. Average Vertical Spectra Normalized by σ^2_{2000} for Three Altitude Bands

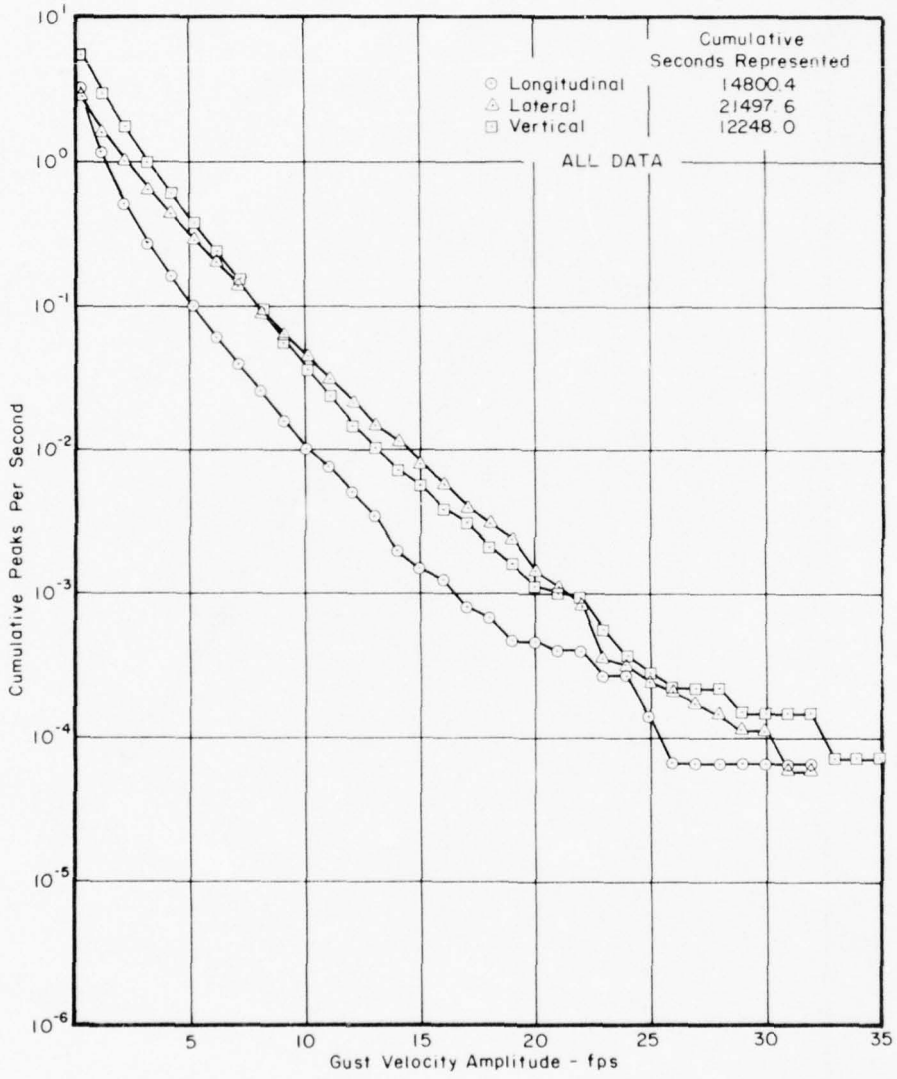

Figure 13. Component Effects on Gust Velocity Peaks

(b) The occurrence rate of the longitudinal components appears to be a constant percentage of the vertical component except at the extreme ends of the amplitude scale.

(c) In the very low amplitude regions, < 2 feet per second, it appears that some noise exists. These data were not altered to correct for this noise.

The cumulative distributions of the observed peaks are compared to the distribution of peaks as specified in Specification MIL-A-8866 (USAF) in Figure 14. The average of the two sets of values P_i and b_i for the altitude bands which span the MEDCAT regime were used. Thus, the MIL-A-8866 (USAF) cumulative distribution was determined by means of the formula:

$$F(x) = \frac{1}{P_1 + P_2}\left[P_1 e^{-x/b_1} + P_2 e^{-x/b_2}\right]$$

$$= \frac{1}{0.0634}\left[0.0625e^{-x/3.45} + 0.0009e^{-x/11.15}\right]$$

Figure 14 indicates that the MIL-A-8866 (USAF) spectrum is significantly more severe than that obtained from the MEDCAT data for all three components.

The commonly used theoretical results of Rice predict the distribution of level crossings of a stationary Gaussian random process. However, level crossing data are not of prime interest in design criteria. Thus, it is of interest to compare the results of level crossing analysis with the results obtained by peak counting and amplitude counting. In order to make comparison of results meaningful, the results were converted into the format of cumulative probability versus amplitude. Plots are presented for each of the gust velocity components using the results from the three counting methods in Figures 15 through 17.

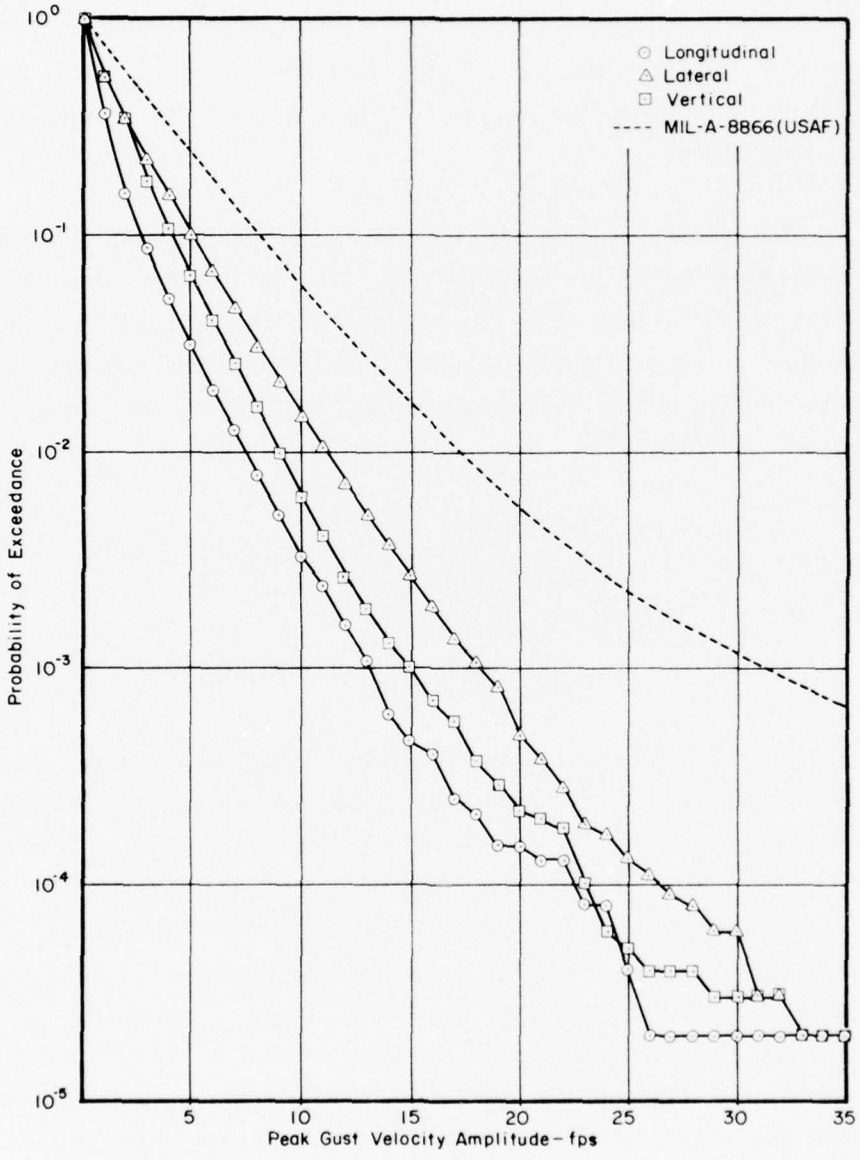

Figure 14. MEDCAT Exceedance Peak Probability vs. MIL-A-8866(USAF)

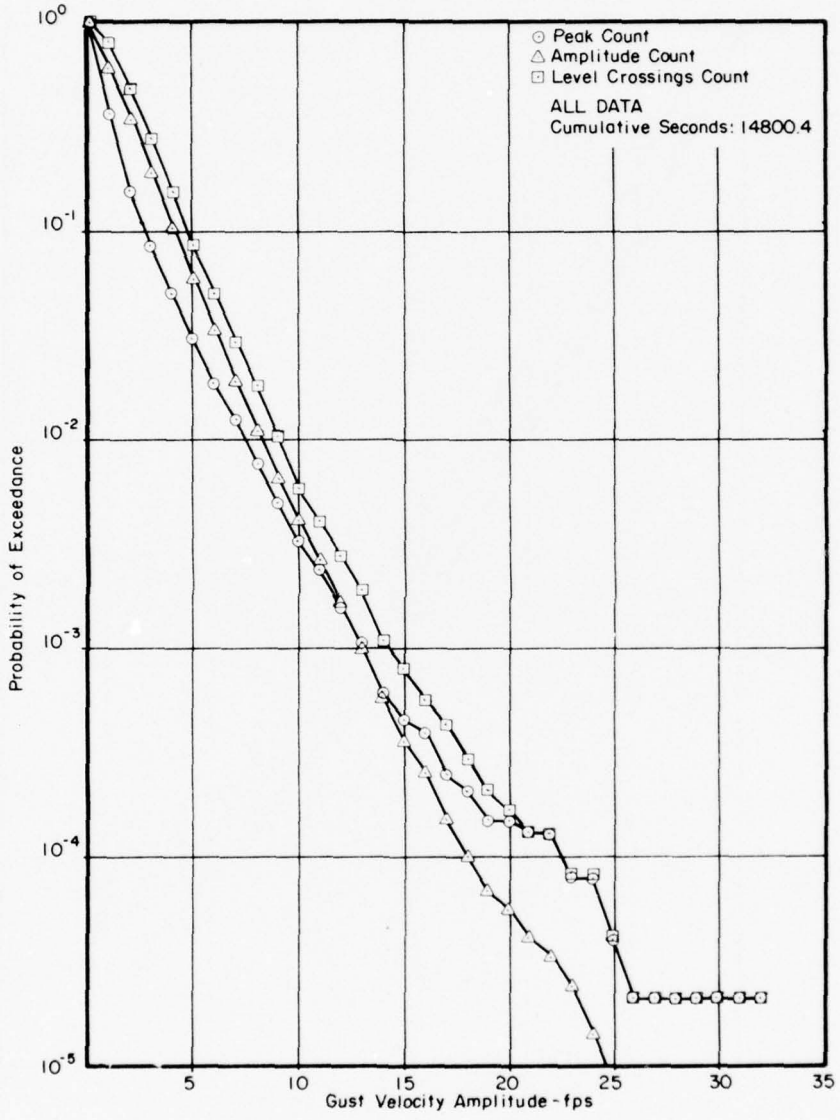

Figure 15. Longitudinal Gust Cumulative Probability Distributions

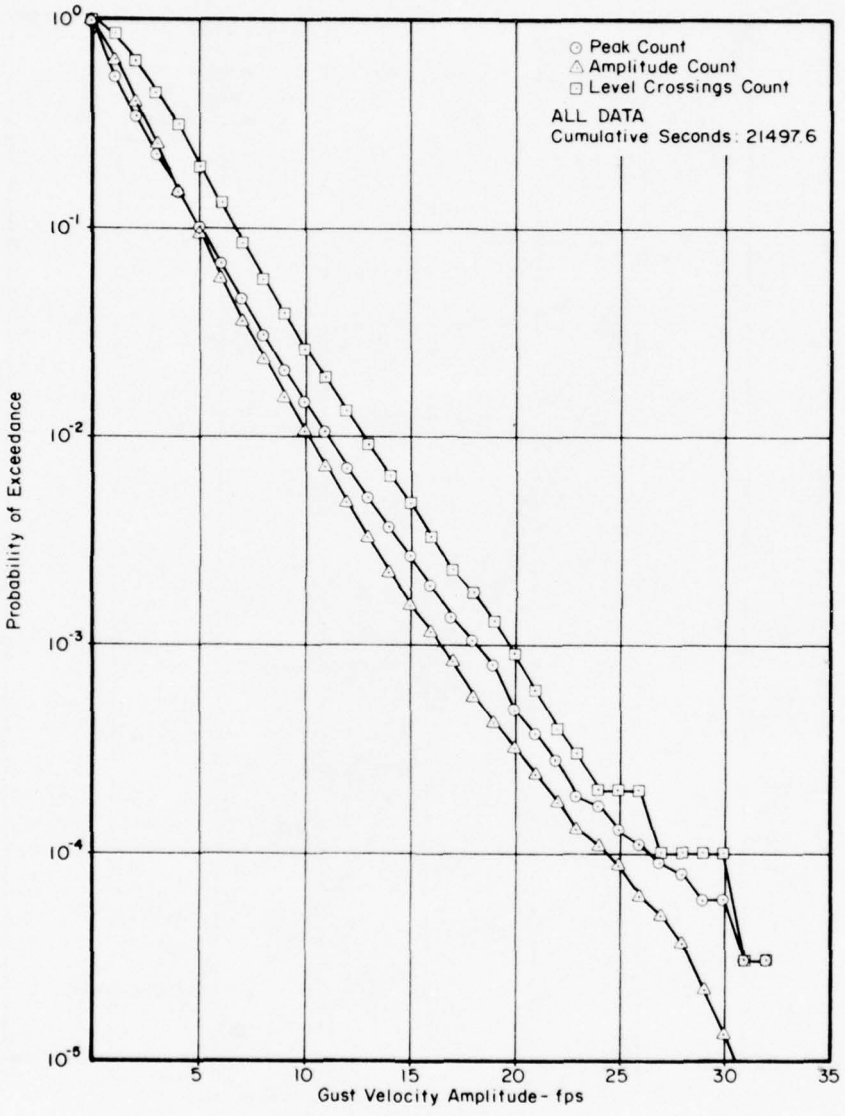

Figure 16. Lateral Gust Cumulative Probability Distributions

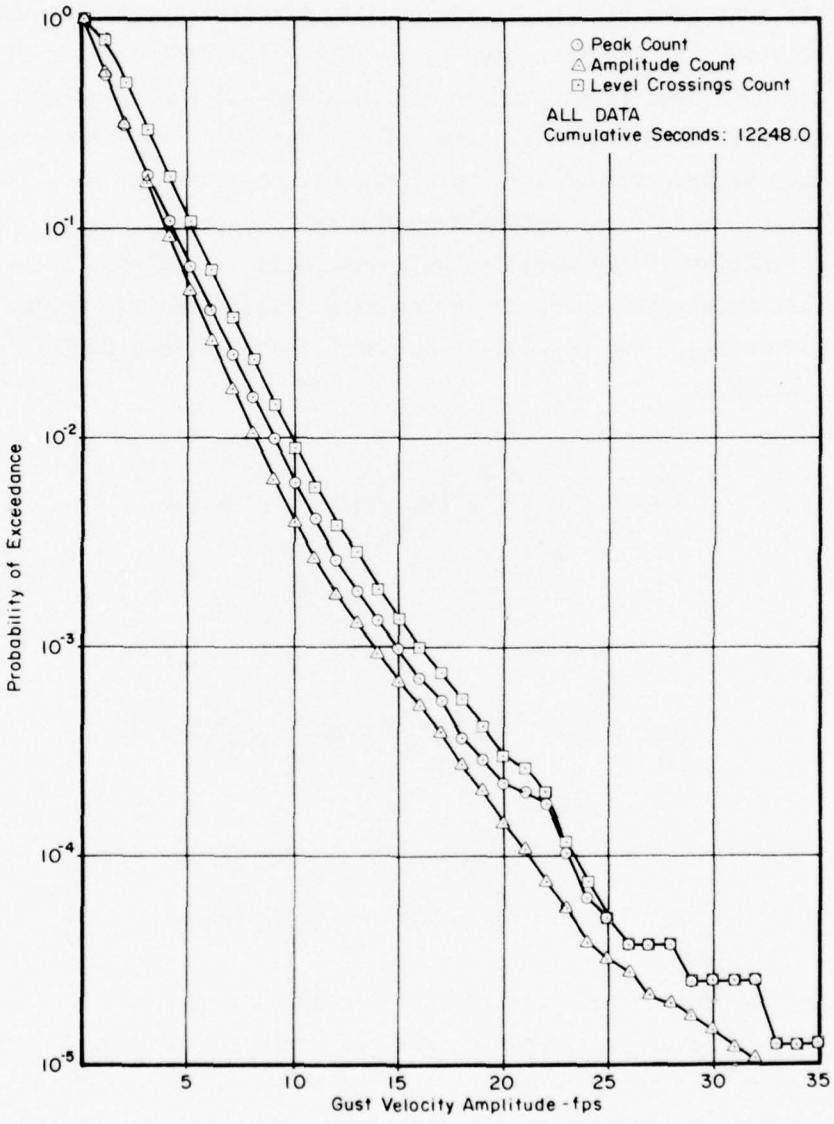

Figure 17. Vertical Gust Cumulative Probability Distributions

A difficulty arises in the evaluation of observed rms values to that present in the evaluation of the scale of turbulence. The rms values desired from the time histories were not comparable since the individual runs were high pass filtered at different cutoff frequencies. It was necessary to use truncated rms values. The distribution of these values did not adequately describe the parameter of the turbulence models as these were stated in terms of σ^2 (not σ^2_λ). The truncated rms values must be transformed into total rms values by accepting a family of theoretical models and determining the ratio of total rms to truncated rms as a function of the model. The investigators used the Taylor-Bullen theoretical models to represent the spectra rather than the Dryden or von Karman models. For the Taylor-Bullen Transverse Family, this can be accomplished by:

$$\sigma^2 k_1 = \sigma^2 \int_{k_1}^{k_o} \phi^*(k,L,m) = \sigma I^2(L,m,k,)$$

and

$$\phi(k) = 2\sigma^2 L \; \frac{[1 + 2\,(n+1)\, b^2\, (2\pi\, kL)^2]}{[1 + b^2 (2\pi\, kL)^2]^{\,n+3/2}}$$

where

$$n = 1/2\ (-m-1) \text{ and } b = \frac{\Gamma(n)}{\sqrt{\pi}\,\Gamma(n + 1/2)}$$

The use of these equations first implies knowledge of m and L. These parameters displayed considerable variation between individual turbulence runs in the MEDCAT data. However, for the purposes of presenting the rms data, it was assumed that L = 3000 feet and m = -1.83 for the lateral component and m = -1.33 for the vertical component.

Histograms of the estimates of σ^2 are presented in Figure 18. In interpreting these higtograms it is important to realize that the editing criteria for the turbulence runs of this figure included the

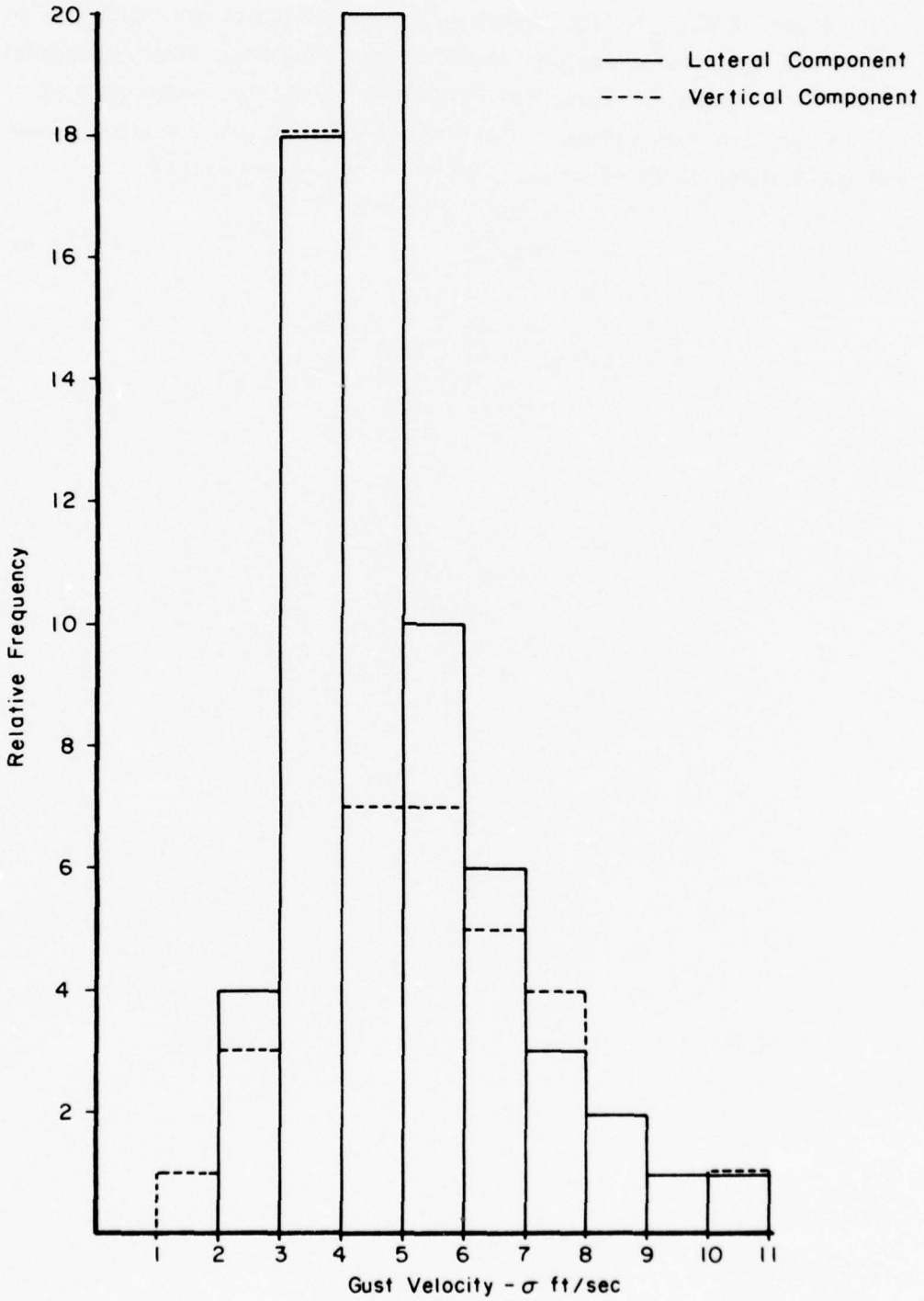

Figure 18. Histogram of Computed Total RMS Values, σ, for Lateral and Vertical Components

requirements that $\sigma_t > 1.5$. Further, in collection of the data, the pilot sought the atmospheric regions predicted as being most likely to contain clear air turbulence. Thus, this histogram cannot be interpreted as a random sample of rms values since the data base is not a random sample and the truncation point of the σ distribution was variable.

SECTION V

PROJECT HICAT

The HICAT program results are based upon flight measurements of aircraft cg acceleration response and the true gust velocity components together with measurements of the related aerodynamic and meteorological variables. HICAT tests involve deliberate flights into regions of turbulence or suspected turbulence. A major objective was to determine gust velocity spectra for turbulence ranging from 100 feet to 50,000 feet in wave length. These flights were designed to sample the variety of atmospheric phenomena associated with turbulence in the 40,000 to 70,000 ft altitude region. This program provides the basic data for the development of a statistical model of world-wide high-altitude clear-air turbulence. The following tabulation from Reference 9 summarizes all the HICAT flight experience including that from the initial and redirected HICAT programs:

HICAT Program	Test Period	Tests	Tests Encountering HICAT	Flight Hours	HICAT Hours
Initial	Feb 64 - Oct 64	33	17	94.5	7.4
Redirected	Oct 65 - Feb 67	146	84	649.5	29.2
Extended	Mar 67 - Feb 68	106	72	477.6	18.3
All	Feb 64 - Feb 68	285	173	1221.6	54.9

An extensive analysis of the meteorological and geophysical conditions with high altitude clear air turbulence was conducted and reported in Reference 10. The distributions of the number of observations by season and latitude are shown in Figure 19. The ratio of flight miles in turbulence to the total flight miles was analyzed as a function of topography. Four categories were defined as follows:

Water
Flatland (local relief differences < 3000 ft.)
Low mountains (local relief differences 3000 to 7000 ft.)
High mountains (local relief differences > 7000 ft.)

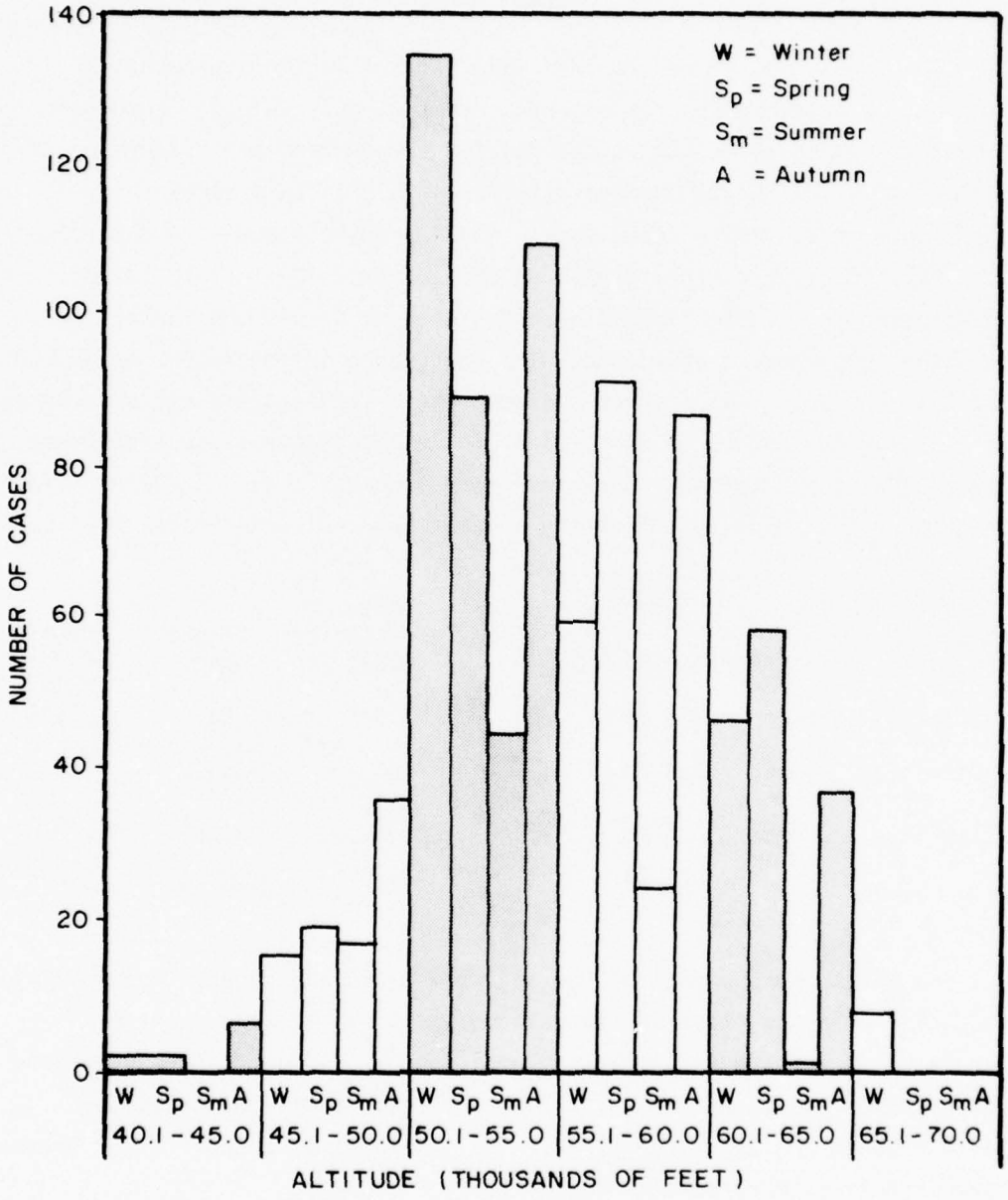

Figure 19. Distribution by Season and Altitude of Number of Observations of High Altitude Clear Air Turbulence

Figure 20 shows the distribution of the number of observations by topography and by season. HICAT data indicate that the percentage of turbulence is related to the topography immediately below the aircraft. Figure 21 presents the distribution of total flight miles and turbulent flight miles by terrain for ferry flights and all flights.

An important objective of the HICAT program was to derive gust velocity spectra for turbulence waves ranging from 100 feet to as much as 50,000 feet in length. To achieve uniform statistical reliability it is required that sample lengths increase in proportion to the largest wavelength of interest in the spectrum. The square root of the integral of the spectral curve from the short wavelength limit to the longest wavelength of interest for the design and operation of aircraft is an important quantity, but one that is rarely obtainable from direct measurements. A method was presented, in References 9 and 11 for comparing spectra with different limits using the root mean square (rms) values for the following wave length limits: 1000, 2000, 4000, 10,000, 20,000, and 40,000 feet. The short wavelength limit was established at 140 feet. The envelopes of minimum wavelengths and maximum wavelengths for turbulence investigations are presented in Figures 22 and 23 from Reference 12.

The ratios of the rms at λ = 2000 ft, λ = 4000 ft, λ = 10,000 ft, and λ = 20,000 ft to rms at λ = 1000 ft were used as quantitative measures of the shape of the spectra. Table 6a presents the average values of these ratios for two categories of topography and for three values of the maximum wavelength of the spectra. Table 6b also includes the calculated ratios for the "mild knee" equation with the slope m of the short wavelength equal to -5/3.

The "mild knee" equation is

$$\Phi(\Omega) = \frac{\text{constant}}{1 + (\Omega L)^{-m}}$$

when Φ (Ω) is the power spectral function, Ω is the reduced frequency ($2\pi/\lambda$) and L is the scale of turbulence. This equation appeared to best fit the HICAT spectra data for the three components of the gust velocity presented in Table 6a.

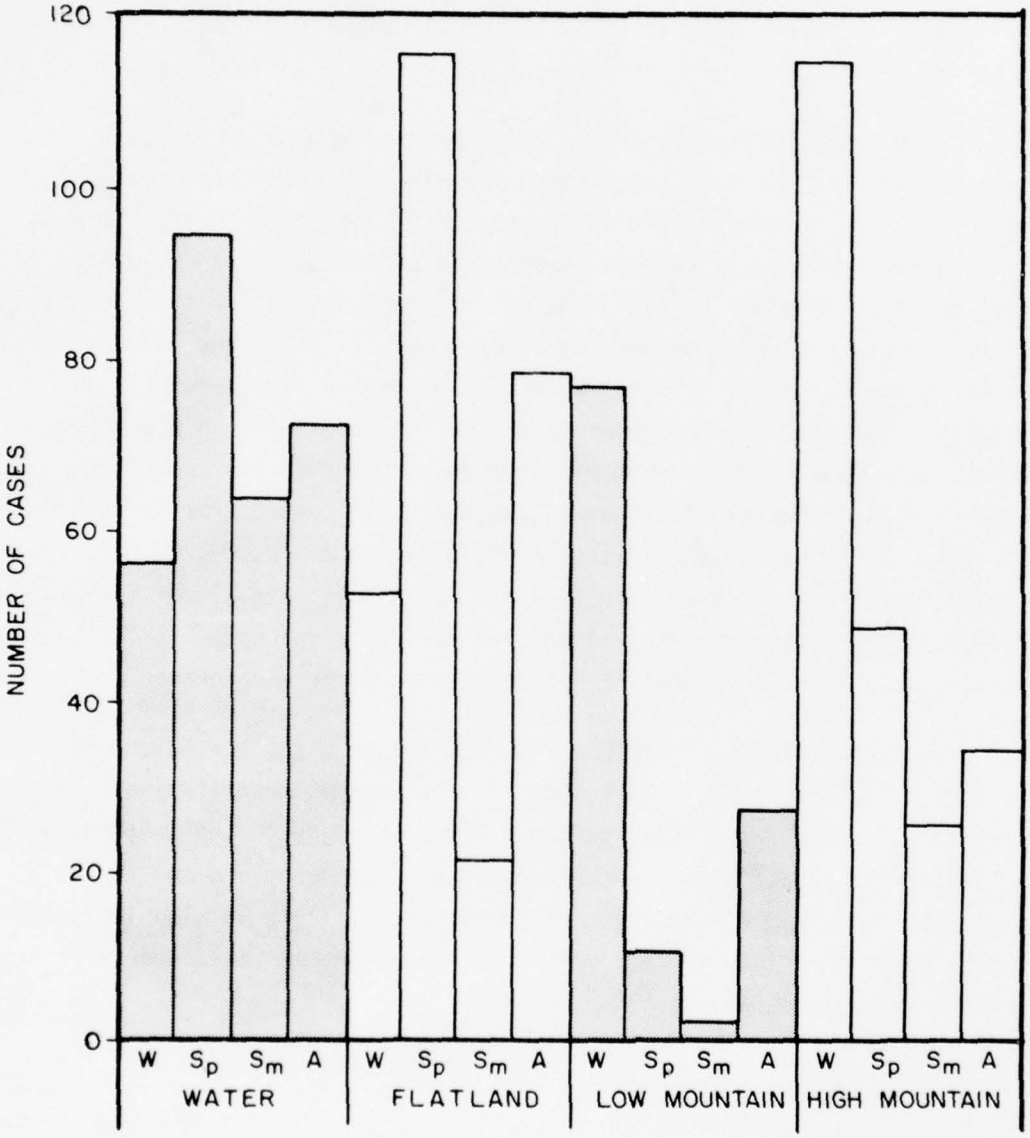

Figure 20. Distribution of the Number of Observations of Turbulence by Topography and by Season

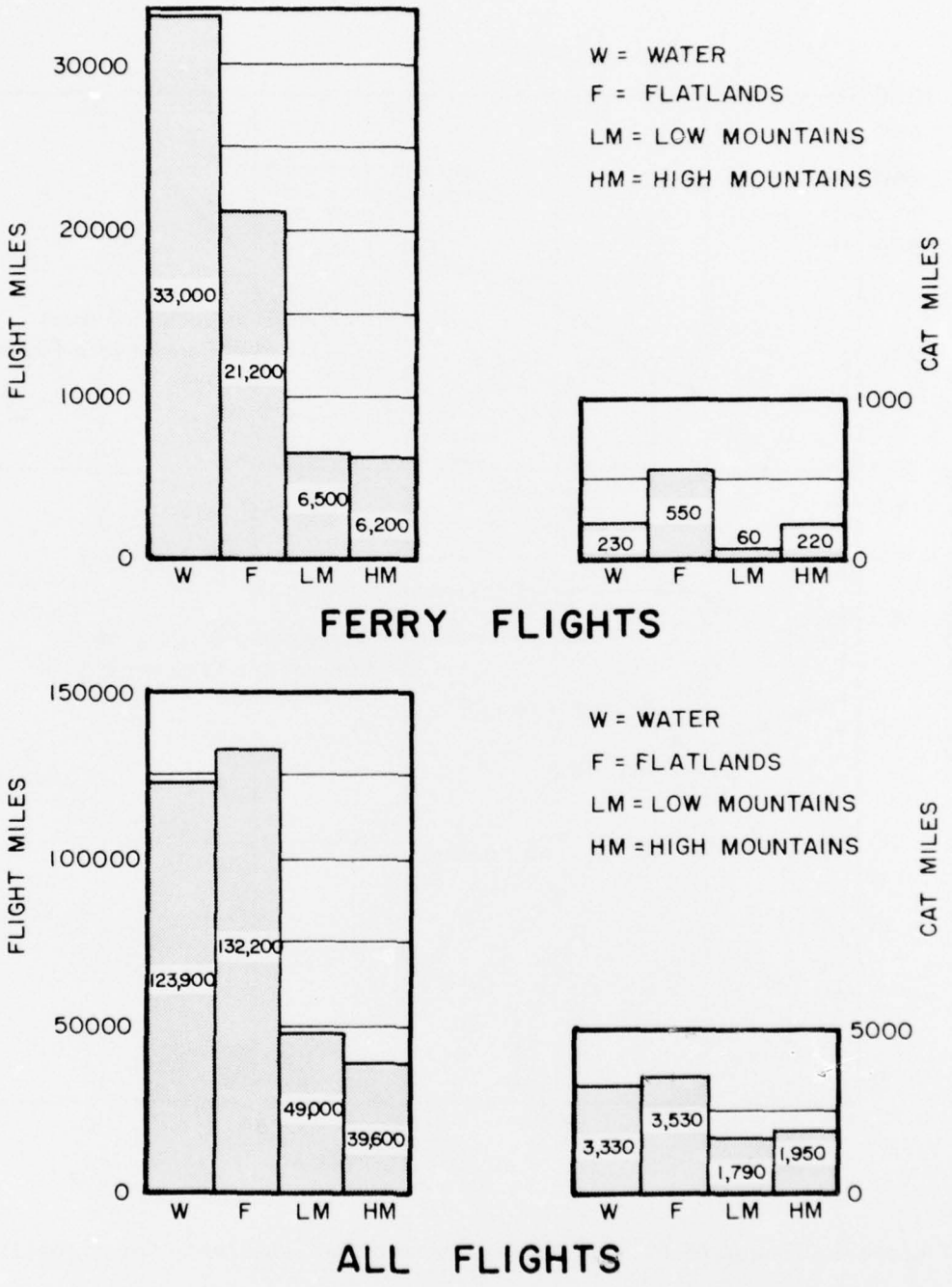

Figure 21. Distribution of Total Flight Miles and Turbulence Flight Miles by Terrain for Ferry Flights and All Flights

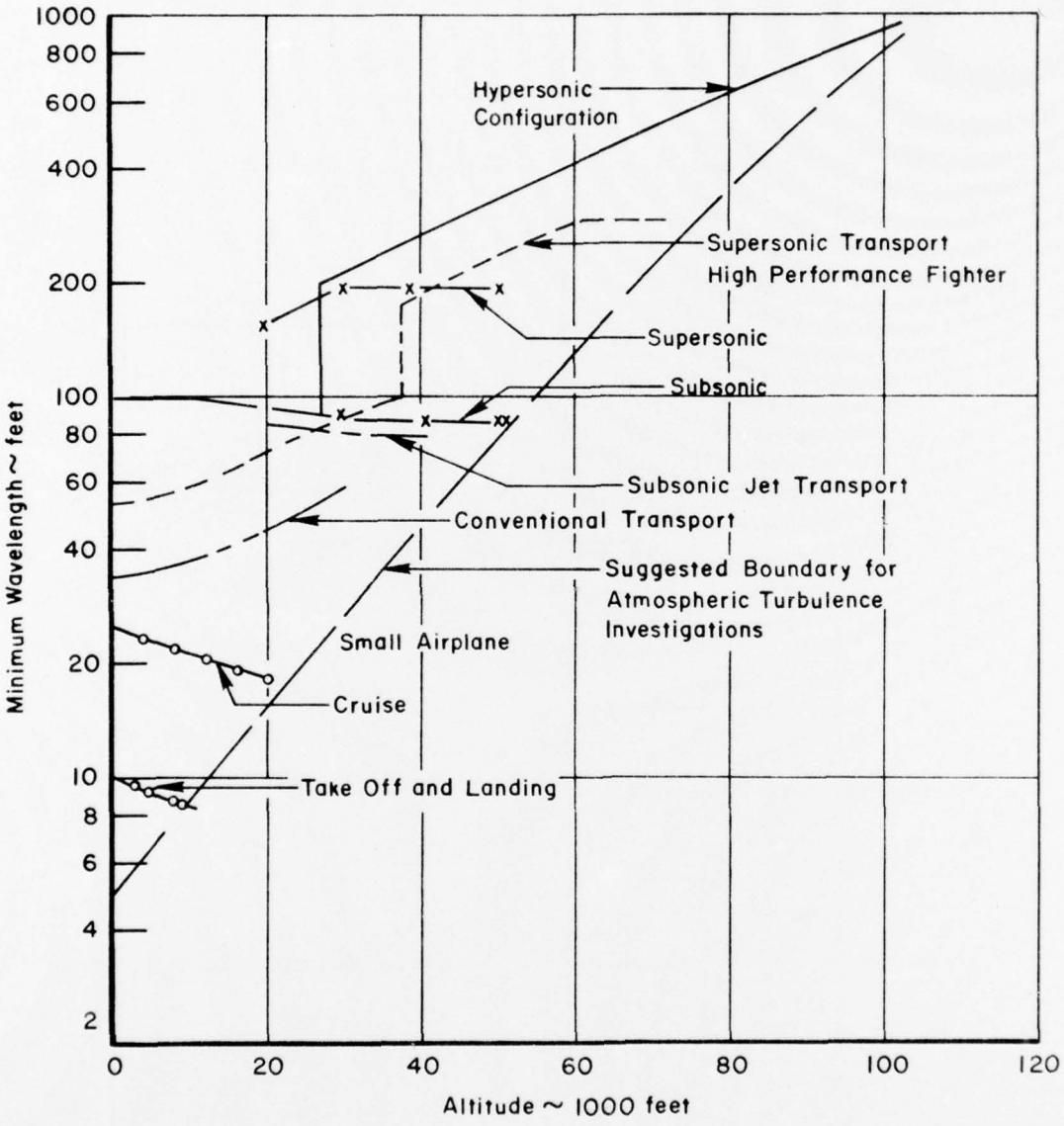

Figure 22. Envelope of Minimum Wavelengths for Turbulence Investigations

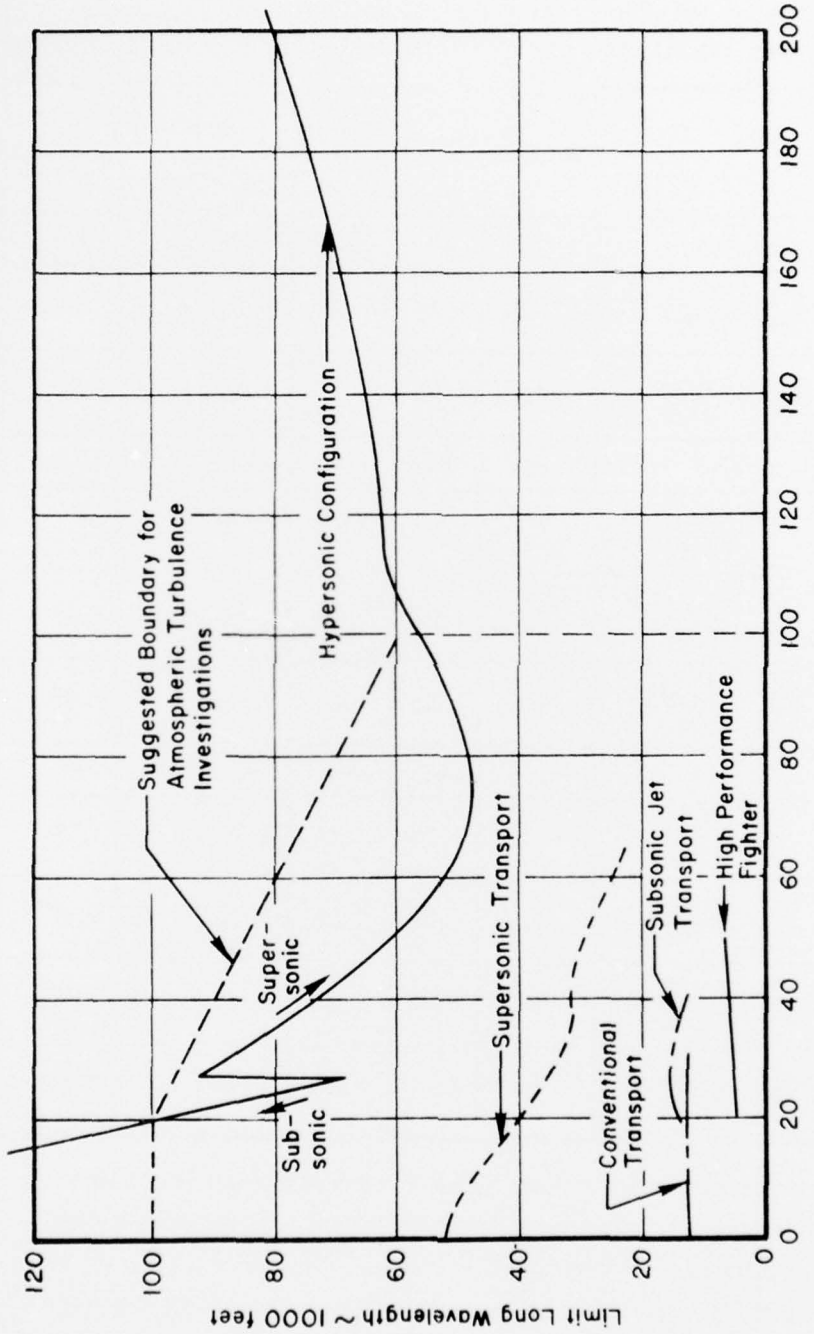

Figure 23. Limit Long Wavelength Variation With Altitude

TABLE 6a

AVERAGE VALUES OF THE RATIO OF U_V, U_F, AND U_L AT RMS (2000), RMS (4000), RMS (10,000), AND RMS (20,000) TO RMS (1000)

		Water, Flatland			Mountains		
		U_V	U_F	U_L	U_V	U_F	U_L
λ max 4000 ft	Samples	(13)	(31)	(44)	(40)	(54)	(55)
	$\frac{\text{RMS (2000)}}{\text{RMS (1000)}}$	1.23	1.26	1.25	1.29	1.32	1.30
	$\frac{\text{RMS (4000)}}{\text{RMS (1000)}}$	1.48	1.57	1.55	1.65	1.69	1.77
λ max 10,000 ft	Samples	(8)	(14)	(16)	(16)	(19)	(20)
	$\frac{\text{RMS (2000)}}{\text{RMS (1000)}}$	1.19	1.25	1.25	1.29	1.32	1.28
	$\frac{\text{RMS (4000)}}{\text{RMS (1000)}}$	1.37	1.52	1.54	1.63	1.67	1.75
	$\frac{\text{RMS (10,000)}}{\text{RMS (1000)}}$	1.65	1.95	1.91	2.06	2.31	2.45
λ max 20,000 ft	Samples	(2)	(4)	(4)	(4)	(5)	(5)
	$\frac{\text{RMS (2000)}}{\text{RMS (1000)}}$	1.21	1.29	1.24	1.31	1.34	1.29
	$\frac{\text{RMS (4000)}}{\text{RMS (1000)}}$	1.36	1.53	1.50	1.72	1.75	1.76
	$\frac{\text{RMS (10,000)}}{\text{RMS (1000)}}$	1.54	1.80	1.71	2.25	2.51	2.50
	$\frac{\text{RMS (20,000)}}{\text{RMS (1000)}}$	1.67	2.01	1.86	2.66	3.19	3.11

A total of 732 samples for which the flight path was level and the turbulence was indicated to be very light were used to determine the distribution lengths of the turbulent regions. The percentages of exceedances were computed for the total sample for cases of moderate or greater turbulence (144 cases) and severe turbulence (16 cases).

TABLE 6b

THEORETICAL VALUES OF THE RATIOS OF RMS (2000), RMS (4000), RMS (10,000) AND RMS (20,000) TO RMS (1000) FOR VARIOUS L'S OF THE MILD KNEE EQUATION WITH m = -5/3						
	Scale Length in Feet					
	500	1000	2000	4000	6000	8000
$\frac{\text{RMS (2000)}}{\text{RMS (1000)}}$	1.23	1.26	1.30	1.32	1.33	1.33
$\frac{\text{RMS (4000)}}{\text{RMS (1000)}}$	1.42	1.48	1.60	1.67	1.72	1.72
$\frac{\text{RMS (10,000)}}{\text{RMS (1000)}}$	1.60	1.78	1.96	2.17	2.25	2.29
$\frac{\text{RMS (20,000)}}{\text{RMS (1000)}}$	1.68	1.92	2.22	2.55	2.58	2.66

The mean lengths of the turbulent regions by altitude interval and season are given in Tables 7 and 8. The data from these tables indicate that the lengths of the turbulent regions decrease with increasing altitude and that the lengths of the turbulent regions are greater in winter than in the other three seasons.

TABLE 7

MEAN LENGTHS OF TURBULENT REGIONS AS A FUNCTION OF ALTITUDE		
Altitude Range	No. of Cases	Mean Length
45,100 - 50,000 ft.	71	24.5 nm
50,100 - 55,000 ft.	299	24.5 nm
55,100 - 60,000 ft.	234	22.0 nm
60,100 - 65,000 ft.	128	17.0 nm

TABLE 8

MEAN LENGTHS OF TURBULENT REGIONS AS A FUNCTION OF SEASON		
Season	No. of Cases	Mean Length
Winter	219	29.5 nm
Spring	196	22.5 nm
Summer	81	22.5 nm
Autumn	236	21.5 nm

In Reference 13, the numerical values for the standard deviation of the rms gust velocities (b_1), the scale lengths and slopes of the power spectral density curves, and the ratio of turbulent flight miles to total flight miles were determined. These numerical values are given in Table 9. The values of b_1 are shown to increase significantly with roughness of terrain for all three components. Numerical values are 0.9 to 3.4 feet per second for the vertical component, 1.5 to 4.6 feet per second for the lateral component, and 1.2 and 4.6 feet per second for the longitudinal component. Table 10 lists the ratios of the turbulent flight miles to total flight miles that are recommended for use in the design and operation of advanced aircraft. The ratios obtained from an analysis of the HICAT data were judged to be high mainly because of the search procedures used.

TABLE 9

VALUES OF s, L, m, b_1 AND $\bar{x}$ FOR HIGH ALTITUDE CLEAR AIR TURBULENCE

	s (ft/sec)			L (ft)			m			b_1 (ft/sec)			$\bar{x}$ (ft/sec)		
Category	Vert.	Lat.	Long.	Vert.	Lat.	Long.	Vert.	Lat.	Long.	Vert.	Lat.	Long.	Vert.	Lat.	Long.
Water	0.46	0.60	0.41	8,000	8,000	16,000	-1.25	-1.50	-1.45	0.9	1.5	1.2	0.95	2.23	2.41
Flatland	0.61	0.79	0.54	8,000	8,000	16,000	-1.25	-1.50	-1.45	1.2	2.0	1.5	0.95	2.21	2.18
Low Mountains	0.86	1.00	0.92	8,000	8,000	16,000	-1.40	-1.70	-1.55	1.9	3.4	3.1	1.11	2.64	2.48
High Mountains	1.25	1.27	1.27	8,000	8,000	16,000	-1.55	-1.75	-1.60	3.4	4.6	4.6	1.37	2.92	2.88
45,000 - 49,900 ft	0.61	0.69	0.48	8,000	8,000	16,000	-1.45	-1.65	-1.55	1.5	2.2	1.6	1.20	2.81	2.74
50,000 - 54,900 ft	0.96	1.03	0.93	8,000	8,000	16,000	-1.45	-1.65	-1.55	2.3	3.3	3.1	1.20	2.94	2.61
55,000 - 59,900 ft	0.90	0.83	0.83	8,000	8,000	16,000	-1.45	-1.65	-1.55	2.2	2.6	2.8	1.20	2.56	2.34
$\geq$ 60,000 ft	1.09	1.20	1.19	8,000	8,000	16,000	-1.45	-1.65	-1.55	2.6	3.8	4.0	1.20	2.37	2.34
All Cases	0.94	0.96	0.91	8,000	8,000	16,000	-1.45	-1.65	-1.55	2.3	3.0	3.0	1.20	2.72	2.48

TABLE 10

RECOMMENDED RATIOS OF TURBULENT FLIGHT MILES TO TOTAL FLIGHT MILES

Category	Ratio Turbulent
65,000-70,000 Ft	0.010
60,000-65,000	0.010
55,000-60,000	0.020
50,000-55,000	0.030
45,000-50,000	0.030
45,000-70,000	0.020
Water	0.018
Flatland	0.018
Low Mountains	0.022
High Mountains	0.030
Winter	0.024
Spring	0.024
Summer	0.014
Autumn	0.018

SECTION VI

CONCLUSIONS

The turbulence data obtained from the ALLCAT Program have been integrated with data from all other available sources to develop improved gust design criteria. Gust design procedures, based on power spectral methods of generalized harmonic analysis, require modeling of the atmospheric turbulence environment in terms of: a spectrum shape, a root-mean-square gust intensity (σ_w), a scale of turbulence (L), and the parameter (P) depicting the proportion of flight time spent in turbulence (see References 14 and 15). Updated P and σ values are presented in Figures 24 and 25. The aircraft response to turbulence is treated in the frequency plane as shown by the equation

$$\phi_x(\omega) = | H_x(\omega) |^2 \phi_w(\omega)$$

which relates the output spectrum of the response variable x to the input spectrum of gust velocities through the frequency response function $H_x(\omega)$, defined as the response x that results from a sinusoidal gust encounter of unit amplitude. This response equation leads to the two basic structural response quantities A and N_o, where A relates the root-mean-square output value σ_x to the root-mean-square gust input σ_w value through the relation

$$\sigma_x = A\sigma_w$$

and N_o defines the number of zero crossings of x with positive slope per second.

Estimates for the turbulence scale L have ranged from 200 ft to over 5,000 ft. The effective scale of turbulence for all altitudes is recommended as L = 750 ft (see Reference 14). The recommended spectrum for the vertical turbulence is the von Karman spectrum.

Load exceedance curves have been established for design based on mission considerations. These updated curves are presented in Figure 26.

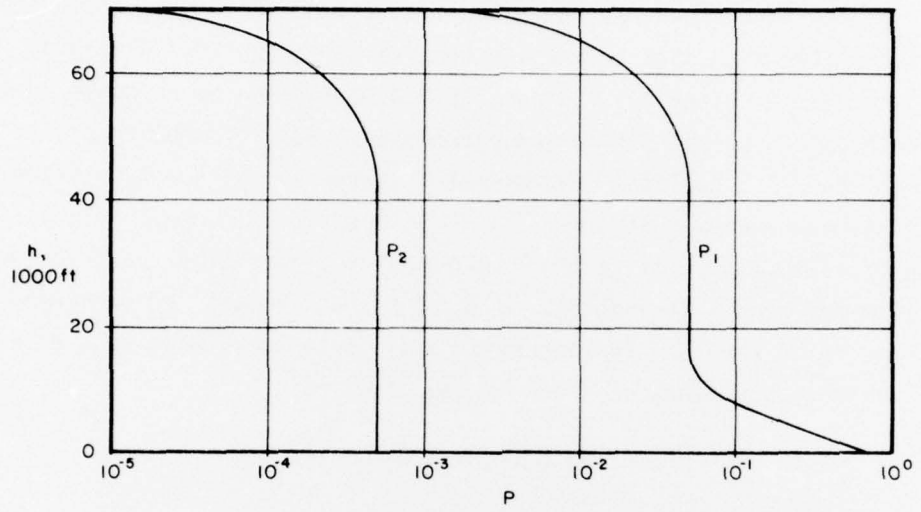

Figure 24. Updated P_1 and P_2 Values

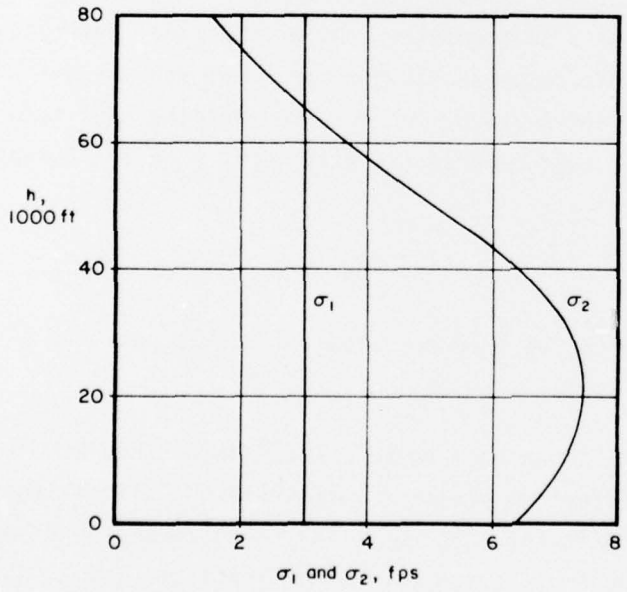

Figure 25. Updated σ_1 and σ_2 Values

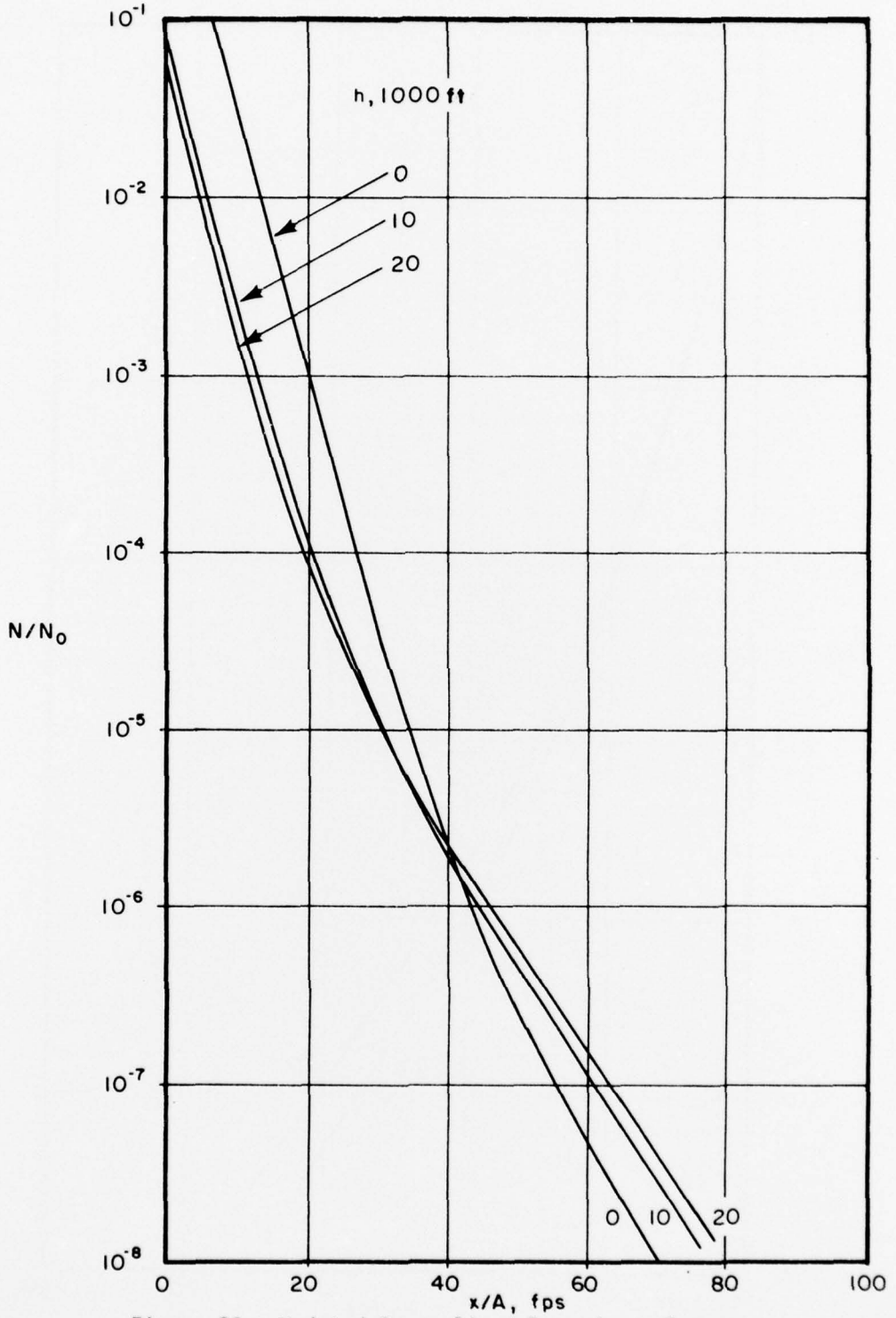

Figure 26. Updated Generalized Exceedance Curves

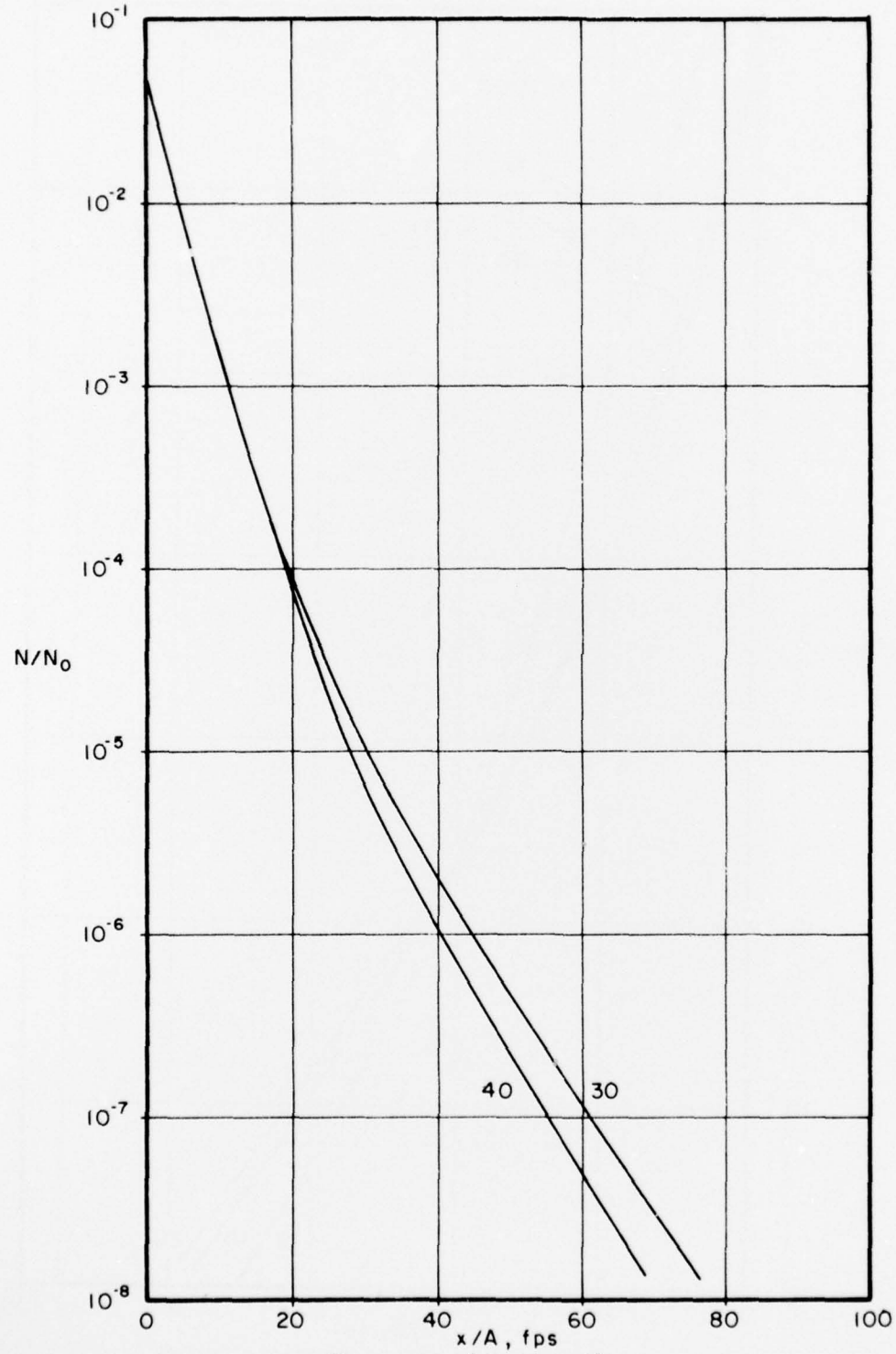

Figure 26. (Continued)

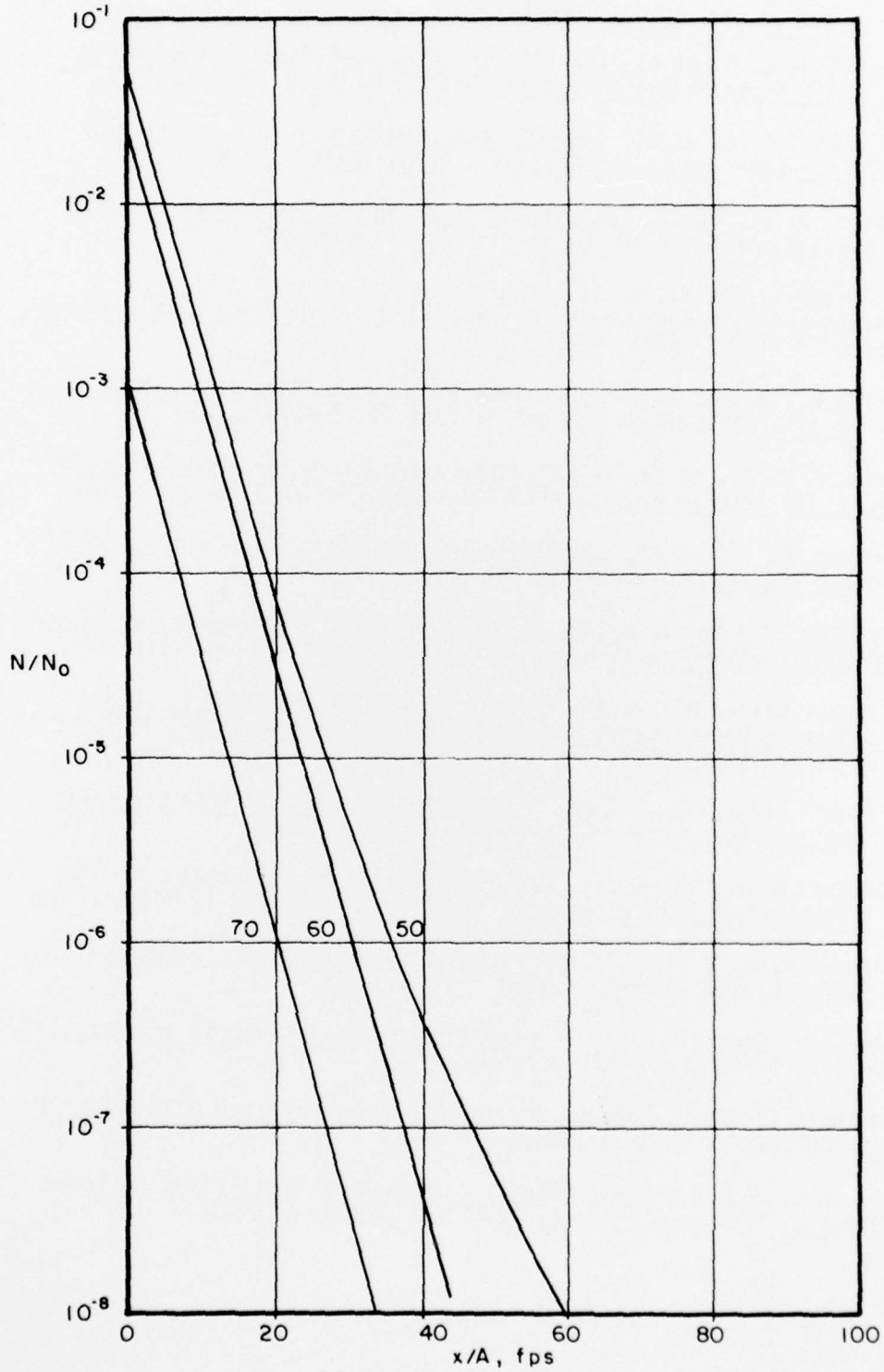

Figure 26. (Concluded)

REFERENCES

1. Elderkin, C. E. et al, Take-Off and Landing Critical Atmospheric (TOLCAT) Experimental Investigation, AFFDL-TR-70-117, May 1971.

2. Elderkin, C. E. et al, Take-Off and Landing Critical Atmospheric (TOLCAT)-Experiments and Analysis, AFFDL-TR-71-172, April 1972.

3. Jones, J. W., et al, Low Altitude Atmospheric Turbulence LO-LOCAT Phase III, AFFDL-TR-70-10, Vol I, Part I, November 1970.

4. McGloskey, John W., et al, Statistical Analysis of LO-LOCAT Turbulence Data For Use In The Development of Revised Gust Criteria, AFFDL-TR-71-29, April 1971.

5. Jones, J. W., et al, Low Altitude Atmospheric Turbulence LO-LOCAT Phase III, AFFDL-TR-70-10, Vol I, Part II, November 1970.

6. Monson, K. R., et al, Low Altitude Atmospheric Turbulence LO-LOCAT Phase III Interim Report, AFFDL-TR-69-63, Volume I, October 1969.

7. Gunter, D. E., et al, Low Altitude Atmospheric Turbulence LO-LOCAT Phases I & II, ASD-TR-69-12, February 1969.

8. Ryan, J. P., et al, Medium Altitude Critical Atmospheric Turbulence (MEDCAT) Data Processing and Analysis, AFFDL-TR-71-82, July 1971.

9. Crooks, Walter M., et al, Project HICAT High Altitude Clear Air Turbulence Measurements And Meteorological Correlations, AFFDL-TR-68-127, Vol I, November 1968.

10. Ashburn, Edward V., et al, Development Of High Altitude Clear Air Turbulence Models, AFFDL-TR-69-79, November 1969.

11. Crooks, Walter M., et al, Project HICAT An Investigation Of High Altitude Clear Air Turbulence, AFFDL-TR-67-123, Vol I, November 1967.

12. Hildreth, W. W. Jr., et al, High Altitude Clear-Air Turbulence, ASD-TDR-63-440, September 1963.

13. Ashburn, Edward V., et al, High Altitude Gust Criteria For Aircraft Design, AFFDL-TR-70-101, October 1970.

14. Houbolt, John C., Updated Gust Design Values For Use With AFFDL-TR-70-106, AFFDL-TR-73-148, November 1973.

15. Houbolt, John C., Design Manual For Vertical Gusts Based On Power Spectral Techniques, AFFDL-TR-70-106, December 1970.

☆ U. S. GOVERNMENT PRINTING OFFICE: 1977 — 757-001/550